UNIVERSIDADE FEDERAL DE SANTA CATARINA
CENTRO DE CIÊNCIAS FÍSICAS E MATEMÁTICAS
PROGRAMA DE PÓS-GRADUAÇÃO EM OCEANOGRAFIA

MARIANE COUCEIRO PULLIG

EVOLUÇÃO MORFOLÓGICA DA DESEMBOCADURA DA BAIA DA BABITONGA, SANTA CATARINA.

FLORIANÓPOLIS
2024

Mariane Couceiro Pullig

EVOLUÇÃO MORFOLÓGICA DA DESEMBOCADURA DA BAIA DA BABITONGA, SANTA CATARINA.

Dissertação submetida ao Programa de Pós-Graduação em Oceanografia da Universidade Federal de Santa Catarina como requisito parcial para a obtenção do título de Mestre em Oceanografia.

Orientador: Prof. Antonio Henrique da Fontoura Klein

Coorientador: Dr. João Thadeu de Menezes

Florianópolis

2024

Ficha catalográfica gerada por meio de sistema automatizado gerenciado pela BU/UFSC.
Dados inseridos pelo próprio autor.

Pullig, Mariane Couceiro
Evolução morfológica da desembocadura da baia da Babitonga, Santa Catarina / Mariane Couceiro Pullig ; orientador, Antonio Henrique da Fontoura Klein, coorientador, João Thadeu de Menezes, 2024.
74 p.

Dissertação (mestrado) - Universidade Federal de Santa Catarina, Centro de Ciências Físicas e Matemáticas, Programa de Pós-Graduação em Oceanografia, Florianópolis, 2024.

Inclui referências.

1. Oceanografia. 2. Desembocadura de maré. 3. Métodos de Interpolação. 4. Delta de maré vazante. 5. Modelo Digital de Elevação. I. Klein, Antonio Henrique da Fontoura. II. de Menezes, João Thadeu . III. Universidade Federal de Santa Catarina. Programa de Pós-Graduação em Oceanografia. IV. Título.

Mariane Couceiro Pullig

Evolução morfológica da desembocadura da baia da Babitonga, Santa Catarina

O presente trabalho em nível de mestrado foi avaliado e
aprovado em 19/12/2023 pelos membros:

Prof., Dr. Jarbas Bonetti Filho
Instituição: Universidade Federal de Santa Catarina

Prof., Dr. Giovanni Coco
Instituição: University of Auckland

Certificamos que esta é a versão original e final do trabalho.

Documento assinado digitalmente
Pedro de Souza Pereira
Data: 13/03/2024 17:31:29-0300
CPF: ***.759.524-**
Verifique as assinaturas em https://v.ufsc.br

Coordenação do Programa de Pós-Graduação

Documento assinado digitalmente
Antonio Henrique da Fontoura Klein
Data: 13/03/2024 17:41:01-0300
CPF: ***.210.710-**
Verifique as assinaturas em https://v.ufsc.br

Prof. Antonio Henrique da Fontoura Klein, Dr.(a)
Orientador(a)

Florianópolis, 2024

À Angela Toscano Couceiro,
que me inspirou a querer aprender.

AGRADECIMENTOS

Agradeço ao CNPQ pelo apoio ao projeto "*Análises dos impactos ambientais e econômico no setor portuário costeiro decorrentes das mudanças do clima: estudos de caso - portos de São Francisco do Sul (setor público) e Itapoá (setor privado), Santa Catarina [Projeto - RiscPorts]"*, de numeração 441545/2017-3, dentro do qual esta dissertação foi desenvolvida.

Agradeço ao Prof. Antonio Henrique da Fontoura Klein pela oportunidade de superação que me foi confiada, pelo direcionamento e atenção ao longo dessa jornada científica, e pelos ensinamentos através dos quais pude me desenvolver.

Agradeço aos pareceristas Dr. Guilherme Vieira da Silva (Griffith University), Prof. Jarbas Bonetti (UFSC), Prof. Eduardo Siegle (USP), Prof. Pedro Pereira (UFSC) pelas dicas e correções ao longo do desenvolvimento do trabalho. Agradeço ao Professor J. Andrew G. Cooper (Ulster University) pela revisão e contribuições ao manuscrito.

Agradeço a BSc. Lais Pool (URGS), Prof. Deivid Leal Alves (UEMS), Dr. João Thadeu de Menezes (Acquadinâmica) e Bsc. Marcos Felipe Tomasi pela coautoria dos artigos e parceria acadêmica.

Agradeço aos colegas do Laboratório de Oceanografia Costeira, do Laboratório de Dinâmica dos Oceanos e do Laboratório de Gestão Costeira e Integrada, em especial PhD Wagner Costa, PhD Tiago Gandra, MSc Mario Mascagni, MSc Wilson Galvão, BSc Gabriela Freire, BSc Larissa Souza e BSc Luiza Fiorini pelas discussões científicas.

RESUMO

As desembocaduras de maré e os promontórios rochosos são componentes integrais de muitos sistemas de deriva litorânea. Embora os mecanismos de transposição de sedimentos em desembocaduras e promontórios tenham sido descritos, a compreensão da conectividade dos sedimentos e do seu processamento em sistemas que combinam promontório e desembocadura é muito limitada. Neste artigo é apresentado um modelo conceitual abordando a evolução morfológica de uma desembocadura controlada por promontório na baía da Babitonga, sul do Brasil. O modelo envolve mudanças de longo prazo nas rotas sedimentares associadas a transposição combinada do promontório e desembocadura. Múltiplos conjuntos de dados batimétricos históricos foram compilados para criar uma base de dados morfológicos de longo prazo, abrangendo um período de 160 anos (1862-1941). Um teste de vários métodos de interpolação identificou o método de interpolação EBK como o mais adequado para reconstruir as feições morfológicas conforme apresentadas em cartas náuticas. As evidências morfológicas apontam que a orientação do canal, ou seja, a configuração do escoamento do fluxo vazante no delta da maré vazante, afeta o mecanismo de transposição. A fase inicial é caracterizada por uma orientação do canal a jusante e transposição do promontório através de regiões próximas da costa, e o transporte residual em direção ao canal resulta na formação de secções estreitas e mais largas ao longo do canal. Devido à variação da geometria ao longo do canal, o fluxo empurra os sedimentos em direção a um complexo de barras intermareais, induzindo a reversão do transporte litorâneo no lóbulo a jusante. Durante a próxima etapa, o fluxo de vazante é redirecionado para o lobo sul, induzindo a distribuição em direção ao mar do sedimento que contorna o promontório e o sedimento transpõe o sistema através dos bancos sobre o delta da maré vazante e lóbulo terminal.

Palavras-chave: Desembocadura de meso-escala, delta de maré vazante, Costa de energia mista, métodos de interpolação, base de dados de Cartas náuticas

ABSTRACT

Tidal inlets and rock headlands are integral components of many longshore drift systems. Although the mechanisms of sediment bypassing at inlets and headlands have been described, the understanding of sediment connectivity and its processing within combined headland/inlet systems is very limited. In this paper a conceptual model is presented addressing the morphological evolution of a headland-controlled inlet at Babitonga bay, southern Brazil. This involves long-term shifts of sedimentary pathways associated with headland-Inlet bypassing. Multiple historic bathymetric datasets were compiled to create a long-term morphological database, spanning a period of 160 years (1862-1941). A test of various interpolation methods identified the EBK interpolation method as the most suitable to reconstruct the morphological features presented in nautical charts. The morphological evidences point that the basin-channel orientation, i.e., outflow configuration onto the ebb tidal delta, affects the headland-inlet bypassing mechanism. The initial stage is characterized by a downdrift basin-channel orientation and nearshore headland bypassing and residual transport towards the channel-basin results in the formation of narrowing and widen sections along the channel. Due to the along-channel variation, the channel scour sediment toward an intertidal bar complex, inducing longshore transport reversal on the downdrift lobe. During the next stage, the ebb flow is redirected toward the southern lobe, inducing the seaward distribution of the sediment that bypasses the headland and sediment is transported through the ebb tidal delta outer shoals.

Keywords: Meso-scale Inlet, Ebb tidal delta, Mixed-energy coast, Interpolation methods, Nautical charts database

RESUMO EXPANDIDO

Introdução

Desembocaduras de maré de meso-escala estão associadas a um grande volume de água que adentra o corpo d'água associado durante o período de enchente de um ciclo de maré. Dessa forma, desembocaduras de maré de meso-escala apresentam depósitos sedimentares e área da secção transversal do canal principal bem desenvolvidos. Em relação à distribuição dos depósitos sedimentares, esses dependem da amplitude da maré, intensidade da corrente longitudinal, aporte sedimentar, energia e direção das ondas e descarga fluvial.

A transposição de sedimentos em torno de desembocaduras de meso-escala de energia mista é um resultado da interação entre as correntes de maré e as ondas. Enquanto as correntes de maré direcionam o sedimento em direção ao mar em períodos de vazante, e em direção as margens do canal em períodos de enchente, as ondas contribuem para o transporte transversal em direção a costa e longitudinal no sentido da corrente litorânea. A transposição de desembocaduras pode influenciar na evolução morfológica de desembocaduras associadas a grandes corpos d'água e/ou com grande amplitude de maré, uma vez que são capazes de reter e eventualmente liberar grandes quantidades de volume sedimentar. Os mecanismos de transposição podem envolver a reorientação do canal principal, o rompimento dos depósitos resultantes da interação de onda e maré (delta de maré vazante), a ruptura de pontais arenosos, o desenvolvimento de bancos, migração em direção a costa e eventual anexação à costa.

A presença de promontórios rochosos associados a desembocaduras introduzem maior dificuldade na compreensão dos mecanismos de transposição de desembocaduras e influência na evolução morfológica desses ambientes. Isso ocorre porque s promontórios podem influenciar na direção das correntes de maré (desviando jatos, por exemplo) e nos processos de ondas, como nos exemplos do fenômeno de refração.

Objetivos

O objetivo geral da presente dissertação é desenvolver um modelo conceitual acerca da evolução morfológica de uma desembocadura de meso-escala controlada por promontório

rochoso. Especificamente, objetiva-se analisar as mudanças morfológicas observadas em dados batimétricos da desembocadura da baia da Babitonga no longo-prazo (1862 a 2021).

Metodologia

Essa dissertação utiliza dados batimétricos extraídos de cartas náuticas e folhas de bordo publicados pela Marinha do Brasil para a geração de Modelos Digitais de Elevação através da interpolação de dados. A performance dos métodos de interpolação Ponderação pelo Inverso da distância, Krigagem ordinária e Krigagem Empírica foi comparada para seleção do mais adequado à representação do relevo submerso da baia da Babitonga. O método Krigagem Baiesiana Empírica foi selecionado para gerar os Modelos Digitais de Profundidade, que foram comparados pela diferença de profundidade, declividade e migração das feições.

Resultados e Discussão

Os resultados do primeiro período de análise (1862-1941) mostraram acumulação sedimentar em meio ao canal, em sua secção sudeste, e variação da largura da secção transversal. Com o desenvolvimento do estágio, essa diferença na largura (geometria) pode ter aumentado a intensidade da corrente vazante, uma vez que o canal passou a ser constrito em determinados pontos. Durante esse período, é provável que o transporte na direção do canal ao redor do promontório tenha dominado. Dessa forma, o sedimento trazido pela corrente de maré vazante em direção ao para o lóbulo sul do delta de vazante é novamente redirecionado ao canal. Isso se deve ao fato de que a "zona de deflecção de fluxo", ou seja, a zona em que a interação entre o promontório e ondas deflete as correntes de maré, encontrava-se mais próximo da entrada da desembocadura.

Conforme o estágio desenvolveu-se, o sedimento que entrava no canal e era direcionado ao lóbulo sul, retornaria ao canal devido a deflecção da corrente de vazante. Por outro lado, as porções constritas (secção nordeste) do canal teriam maior tendência a ser defletidas para nordeste, acumulando-se marginalmente na barra marginal de Galharada.

No próximo período (1941 – 1972) observou-se a diminuição dos depósitos em meio ao canal, ampla sedimentação nos bancos de vazante e a formação de um complexo intermareal no lóbulo norte, Galharada. Além disso, observou-se o aprofundamento da porção do canal mais

interna e o avanço lateral do pontal do Capri. A medida em que os depósitos em meio ao canal são direcionados ao pontal do Capri, este se desenvolve lateralmente e constringe o canal em sua porção mais interna, que passa a redistribuir seu sedimento para a porção do canal mais a updrift e para a barra linear marginal de Galharada. Nesse momento, a área inter-maré chega em seu ápice. Nesse estágio, é provável que a "zona de deflecção de fluxo" tenha se distanciado da entrada da desembocadura, uma vez os depósitos foram liberados. O mecanismo associado a transposição do promontório-desembocadura passa a sofrer influência maior do fluxo vazante, uma vez que o canal alinha-se a costa a montante, paralelamente ao pontal do Capri, a medida em que sua porção mais interna aprofunda-se e este curva-se. Nesse período os depósitos em meio ao canal dão lugar a um único depósito, no interior da curva do canal. Esse período inaugura um estágio de armadilhamento de sedimentos no delta de maré vazante, uma vez que a área intermareal induz o aumento do processo de refração e reversão do transporte longitudinal.

No período entre 1972 e 2021 pode ter ocorrido a dominância do mecanismo de transposição do promontório-desembocadura através da plataforma de vazante e ao longo do lobo terminal do delta. Nesse período ocorre o aprofundamento do lóbulo sul e norte do delta de maré vazante e o aumento da largura do canal, principalmente na direção da margem sudeste. Isso sugere que uma configuração específica de canal, provavelmente devido a formação de um braço sul do canal vazante, e o consequente afastamento em direção ao mar da "zona de deflecção de fluxo", podem ser necessários para que os sedimentos alcancem regiões além da célula de recirculação do delta de maré vazante.

Considerações finais

A presente dissertação apresenta um modelo conceitual de três estágios de evolução morfológica de desembocaduras controladas por promontório. Os estágios basearam-se na evolução morfológica da desembocadura da baía da Babitonga através de dados batimétricos extraídos de cartas náuticas antigas, folhas de bordo e levantamento hidrográficos recentes ao longo de 160 anos (1862-1941). O modelo conceitual propõe a "zona de deflexão de fluxo", cuja posição afeta o mecanismo dominante de transposição sedimentar do promontório-desembocadura.

Palavras-chave: Desembocadura de meso-escala, delta de maré vazante, Costa de energia mista, métodos de interpolação, base de dados de Cartas náuticas

LISTA DE FIGURAS

LISTA DE TABELAS

LISTA DE ABREVIATURAS E SIGLAS

CHM – Centro de Hidrografia da Marinha

BNDO – Banco Nacional de Dados Oceanográficos

SFS – São Francisco do Sul

SUMÁRIO

1 INTRODUÇÃO

Desembocaduras de meso-escala são tipicamente associadas a grandes prismas de maré, e apresentam deltas de maré e área da secção transversal bem desenvolvidos, especialmente em costas dominadas por marés, mas também ao longo de costas dominadas por ondas (O'Brien, 1931; Oertel, 1975; Walton; Adams, 1976). A distribuição dos depósitos sedimentares depende da amplitude das marés, do fluxo de energia litorâneo, da energia das ondas e da descarga fluvial (Hayes, 1979; Oertel, 1975; Walton; Adams, 1976). Enquanto as correntes de maré erodem continuamente o canal, as ondas transportam sedimentos das margens adjacentes para a desembocadura (Oertel, 1979). Como resultado da interação entre ondas e marés, a entrada pode ser classificada como de energia mista, dominada por ondas, ou dominado marés (Davis; Hayes, 1984).

Em deltas de maré vazante dominado por ondas, os processos de onda, como empinamento e quebra de onda, contribuem para a transposição dos sedimentos depositados em bancos submersos para a costa, através do transporte transversal. O processo de migração dos bancos em direção a costa ocorre episodicamente e resulta na coalescência dos bancos e adesão à costa. As ondas também causam movimento ao longo da costa pelo transporte contínuo através do lóbulo terminal do delta de vazante. O processo de transposição sedimentar de desembocadura ocorre através da migração episódica de bancos na maioria dos modelos conceituais apresentados por FitzGerald, Kraus e Hands (2000), enquanto transposição de sedimentos ao longo do lobo terminal do delta está associado a desembocaduras dominadas por ondas. O tamanho do complexo de barras que eventualmente é incorporado ao longo da costa adjacente é diretamente influenciado pelo tamanho da desembocadura (Fitzgerald, 1982). Desta forma, as desembocaduras de meso-escala desempenham um papel crucial no balanço de sedimentos. As desembocaduras aprisionam temporariamente grandes volumes de sedimentos e, eventualmente, os liberam de volta para as porções costeiras adjacentes. Consequentemente, o processo de transposição sedimentar associado às desembocaduras de meso-escala controla uma quantidade significativa do volume de sedimentos e é importante ser levado em consideração na gestão costeira (FitzGerald, 1988).

Múltiplos mecanismos de transposição influenciam na evolução das desembocaduras em costas de energia mista. Os estágios de transposição podem envolver migração da desembocadura, desenvolvimento de bancos e migração para a costa, reorientação do canal, ruptura de delta de maré vazante, ruptura de pontal e anexação de complexo de bancos à costa (FitzGerald 1979; FitzGerald, 1988; Elias; Van Der Spek, 2006) A transposição em torno das desembocaduras de energia mista ocorre através da formação de bancos submersos resultantes da interação maré-onda. As correntes de maré vazante redirecionam os sedimentos em direção ao mar, enquanto o fluxo marginal de enchente é responsável pelo transporte em direção à costa ao longo das laterais do canal de vazante principal. Onde o fluxo de vazante encontra uma força oposta imposta pelas correntes induzidas por ondas orientadas para a costa, os sedimentos são depositados na porção distal do delta de vazante (FitzGerald, 1982). Nas porções do delta de vazante dominadas pelas marés, os fluxos de vazante e de enchente evadem-se lateralmente, formando bancos lineares (Leuven, 2019). A ação das ondas também contribui para a suspensão de sedimentos durante períodos de enchente, levando à distribuição dos sedimentos ao longo dos flancos do canal de vazante (FitzGerald, 1982).

A presença de afloramentos rochosos e promontórios também pode modificar a morfologia e distribuição dos corpos de areia nas desembocaduras, proporcionando áreas abrigadas e realinhando os jatos de vazante, influenciando nos processos de ondas e marés (Hicks e Hume, 1996). Um obstáculo rochoso acrescenta complexidade à transposição de desembocaduras de energia mista, pois introduz um mecanismo de transposição de promontório junto com os processos associados à desembocadura.

Num modelo puro que descreve a transposição sedimentar do promontório, a areia move-se em torno do promontório impulsionada pelas ondas como uma barra que se estende ao redor do promontório em águas rasas, promovendo a transposição para a costa a jusante (Ribeiro, 2017; Klein *et al*., 2020). A areia também pode ser transportada ao redor do promontório em direção ao mar, mas ainda dentro da profundidade de fechamento, como uma barra alongada que fornece um pulso de areia para a costa a jusante à medida que se funde com o compartimento costeiro (Short; Masselink, 1999; Ab Razak, 2015; Klein *et al*., 2020). Outra via de transposição do promontório pode ocorrer desde a praia à montante até águas mais profundas ao largo da costa do promontório. Os processos de formação de ondas transportam

então a areia obliquamente através da praia a jusante da baía (promontório contornando a baía transversal) (Ab Razak, 2015; Vieira da Silva *et al*., 2016).

Embora Fitzgerald, Kraus e Hands (2000) tenha apresentado vários mecanismos de transposição sedimentar de desembocaduras, o conhecimento da dinâmica ao longo de desembocaduras de meso-escala controladas por fronteiras rochosas permanece limitado. Vários estudos de caso avaliaram processos sedimentares em desembocaduras de meso-escala (Elias; Van Der Spek, 2006; Byrnes; Berlinghoff; Griffee, 2013; FitzGerald *et al*., 2000; Calliari *et al*., 2009; Pianca; Holman; Siegle, 2014). Recentemente, Elias *et al*. 2022 combinaram levantamentos batimétricos e observações hidrodinâmicas para descrever a evolução da enseada de Ameland. Na Carolina do Norte, EUA, um modelo baseado em processo foi utilizado para descrever a evolução morfológica da enseada de Oregon em resposta à ação humana

1.1 PERGUNTAS DE PESQUISA

- Qual a influência da evolução morfológica no mecanismo associado de transposição sedimentar do promontório e desembocadura da baia da Babitonga?
- Como a morfologia da desembocadura da Babitonga responde a intervenções de dragagem, e quais as implicações isso tem para sua evolução e mecanismos de transposição sedimentar?
- Como pode ser descrito um modelo conceitual de evolução morfológica natural de uma desembocadura controlada por promontório tendo em vista mudanças na orientação do fluxo vazante?

1.2 OBJETIVOS

1.2.1 Objetivo Geral

Estabelecer um modelo conceitual acerca da evolução morfológica de uma desembocadura de meso-escala controlada por promontório rochoso, através das mudanças

observadas em dados batimétricos da desembocadura da baia da Babitonga no longo-prazo (1862 a 2021).

1.2.2 Objetivos Específicos

- Descrever as mudanças morfológicas no canal principal, canal vazante no delta de maré vazante, canais marginais de enchente e no delta de maré vazante da desembocadura da Babitonga ao longo de 1862-2021;
- Propor um modelo conceitual de evolução que considere a combinação de transposição sedimentar de promontório e desembocadura, levando em consideração a orientação do canal em relação ao delta de maré vazante;

1.2.3 Formato da Dissertação

Esta dissertação apresenta os resultados, discussões e conclusões em forma de artigo, intitulado “Bypassing at a headland-controlled tidal inlet”, a ser submetido à revista Geomorphology (Qualis A1 CAPES/ Area Geociências). Previamente apresenta-se a introdução, as perguntas de pesquisa, e os objetivos da pesquisa. Ao final, são apresentadas as secções discussão geral, Conclusões gerais e Contribuições Científicas, as referências e apêndices.

Mariane Couceiro Pullig

2 BYPASSING AT A HEADLAND-CONTROLLED TIDAL INLET

Esta seção é destinada a apresentação do artigo científico submetido à revista Geomorphology, como parte dos requisitos para a obtenção do grau de mestre em Oceanografia pela Universidade Federal de Santa Catarina.

Florianópolis
2023

Bypassing at a headland-controlled tidal inlet

Mariane Couceiro Pullig[1], Antonio Henrique da Fontoura Klein[1], Laís Pool da Silva Freitas[2], Deivid Cristian Leal Alves[3], João Thadeu de Menezes[4]

Affiliations

1 Federal University of Santa Catarina, University Campus - Trindade, Florianópolis, Santa Catarina, Brazil.

2 Federal University of Rio Grande do Sul, Porto Alegre, Rio Grande do Sul, Brazil.

3 State University of Mato Grosso do Sul, Dourados, Mato Grosso do Sul, Brazil.

4 ACQUADINÂMICA Modelagem e Análise de Risco Ambiental, Balneário Camboriú, Santa Catarina, Brazil.

2.1 ABSTRACT

Tidal inlets and rock headlands are integral components of many longshore drift systems. Although the mechanisms of sediment bypassing at inlets and headlands have been described, the understanding of sediment connectivity and its processing within combined headland/inlet systems is very limited. In this paper a conceptual model is presented addressing the morphological evolution of a headland-controlled inlet at Babitonga bay, southern Brazil. This involves long-term shifts of sedimentary pathways associated with headland-Inlet bypassing. Multiple historic bathymetric datasets were compiled to create a long-term morphological database, spanning a period of 160 years (1862-1941). A test of various interpolation methods identified the EBK interpolation method as the most suitable to reconstruct the morphological features presented in nautical charts. The morphological evidences point that the basin-channel orientation, i.e., the outflow configuration onto the ebb tidal delta, affects the headland-inlet bypassing mechanism. The initial stage is characterized by a downdrift basin-channel orientation and nearshore headland bypassing and residual transport towards the channel-basin results in the formation of narrowing and widen sections along the channel. Due to the along-channel variation, the channel scour sediment toward an intertidal bar complex, inducing longshore transport reversal on the downdrift lobe. During the next stage, the ebb flow is redirected toward the southern lobe, inducing the seaward distribution of the sediment that bypasses the headland and sediment is transported through the ebb tidal delta outer shoals.

Keywords: Meso-scale inlet. Ebb tidal delta. Mixed-energy. Interpolation methods. Nautical charts database

2.2 INTRODUCTION

Meso-scale tidal inlets are typically associated with a large tidal prism they often feature well-developed tidal deltas and large inlet throat cross-sectional area, especially on tide-dominated coasts but also along wave-dominated coasts (O'Brien, 1931; Oertel, 1979; Walton and Adams, 1976). The distribution of sand deposits depends on tidal range, longshore energy flux, wave energy, and fluvial discharge (Hayes, 1975; Oertel, 1975; Walton; Adams, 1976). While tidal currents continuously scour the inlet, waves transport sediment from adjacent shores to the inlet (Oertel, 1975). As a result of wave and tidal interaction, the inlet can be classified as wave- or tide-dominated or mixed energy (Davies; Hayes, 1984). The presence of rock outcrops and headlands can also modify the morphology and distribution of sand bodies in inlets by providing sheltered areas and realigning ebb jets, influencing wave and tidal processes (Hick and Hume, 1996). This means that in a headland-controlled inlet, even on a wave-dominated coast, the coastal morphology can create a mixed energy inlet.

In wave-dominated ebb deltas wave processes, such as shoaling and breaking, contribute to sediment bypassing by cross-shore transport of sand from subtidal bars to the coast. The process of onshore bar migration occurs episodically, and results in bar coalescence and welding to the coastline. Wave processes also cause long-shore movement by continuous transport through the ebb delta terminal lobe. Bypassing through episodic bar migration occurs in most of the conceptual models presented by FitzGerald, Kraus and Hands (2000) while sediment bypassing along the delta terminal lobe is associated with wave-dominated inlets. The size of the bar complex that is eventually incorporated along the adjacent coastline is directly influenced by the size of the inlet (FitzGerald, 1982). In this manner, meso-scale inlets play a crucial role in the coastal sediment budget. They temporary sinks large volumes of sediment and eventually released it back into the adjacent shorelines. Consequently, the bypassing process associated with meso-scale inlets control a significant amount of the sediment volume and is important to coastal management decisions (FitzGerald, 1988).

Several bypassing mechanisms influence on inlet evolution on mixed energy coasts. The bypassing stages may involve inlet migration, swash bar development and onshore displacement (stable inlet model), channel reorientation, ebb tidal delta breaching, spit breaching and the attachment of complexes to adjacent shorelines (Oertel, 1975; FitzGerald, 1988; Elias; Van Der Spek, 2006). Bypassing around mixed energy inlets occurs through the formation of subtidal bars resulting from tide-wave interaction. Ebb tidal currents redirect the sediment seaward, while the marginal flood flux is responsible for landward transport along the

sides of the main ebb channel. Where the ebb flux encounters an opposite force imposed by landward oriented wave-induced currents sediment is deposited in the distal portion of the ebb tidal delta (FitzGerald, 1982). In tidally- dominated portions of the ebb delta, the ebb and flood flows evade each other laterally, forming linear sand bars (Leuven, 2019). Wave action also contributes to sediment suspension during flood transport, leading to landward-oriented sediment motion along the main ebb channel flanks (FitzGerald, 1982).

A rocky obstacle adds complexity on mixed-energy inlets bypassing as it introduces headland bypassing mechanism alongside the inlet-associated processes. In a pure headland bypassing swash-surf zone model, sand moves around the headland via wave-driven longshore drift as a bar extending around the headland within shallow water, promoting bypassing to downdrift coast (Duarte; Taborda; Ribeiro, 2019; Ribeiro, 2017). The sand can also be transported around the headland seaward of the surf zone, but still within the closure depth, as an elongated spit that provides a pulse of sand to the shoreline as it merges with the downdrift compartment (headland bypassing surfzone-nearshore) (Ab Razak, 2015; Short; Masselink, 1999). Another headland bypassing pathway may occur from the updrift beach to deeper water offshore of the headland. The wave shoaling processes then transport sand obliquely across the embayment's downdrift beach (headland bypassing cross embayment) (Ab Razak, 2015; Vieira da Silva *et al*. 2016).

Even though FitzGerald, Kraus and Hands (2000) have presented several mechanisms of inlet sediment bypassing, the knowledge of sediment connectivity and its dynamics along rock boundary-controlled inlets remains limited. Several case studies assessed sedimentary processes at meso-scale inlets (FitzGerald *et al*. 2000; FitzGerald *et al*., 2004; Elias; Van der Spek, 2006; Calliari *et al*. 2009; Byrnes; Berlinghoff; Griffee, 2013; Pianca; Holman; Siegle, 2014). Recently, Elias *et al*. (2022) combined bathymetric surveys and hydrodynamic observations to describe the Ameland Inlet evolution. In North Carolina, US, a process-based model was utilized to describe the morphological evolution of Oregon Inlet in response to human intervention (Velasquez-Montoya; Overton; Sciaudone, 2020). Nonetheless, studies of this kind are infrequent due to the requirement for an extensive, long-term bathymetric database. This study investigates the changes in morphology in Babitonga inlet over the 1862-2021 period, regarding its influence on headland-inlet bypassing.

2.3 REGIONAL SETTING

Situated in Southern Brazil, Santa Catarina State has a microtidal, east-swell, headland-bay coast (Klein; Menezes, 2001), with northerly sedimentary transport (Siegle and Asp, 2007). The Babitonga Inlet-Bay system is located in a strand plain-estuarine depositional setting sector of Santa Catarina's coast (Klein; Menezes, 2001).

The Babitonga estuarine system is of importance on a regional and national scale due to its ecologic, and socio-economic contribution (Cremer, *et al*. 2006). It comprises the largest mangrove area in the state (Vieira *et al*., 2008), and two of the major Brazilian harbors, São Francisco do Sul (SFS) Harbor and Itapoá Harbor. Additionally, the estuary is surrounded by the biggest city of Santa Catarina State, Joinville (Fig. 1).

Figure 1 – Study site (1) Location of Santa Catarina State in Brazil, (2) Location of estuarine system of Babitonga Bay in the State, (3) Location of inlet in the estuary, (4) Inlet's main features. Contour extracted from Brazilian Navy's nautical chart published in 2017. Sediment transport direction from Silveira *et al.* (2012). The thickness of the arrows is not related to the magnitude of the transport.

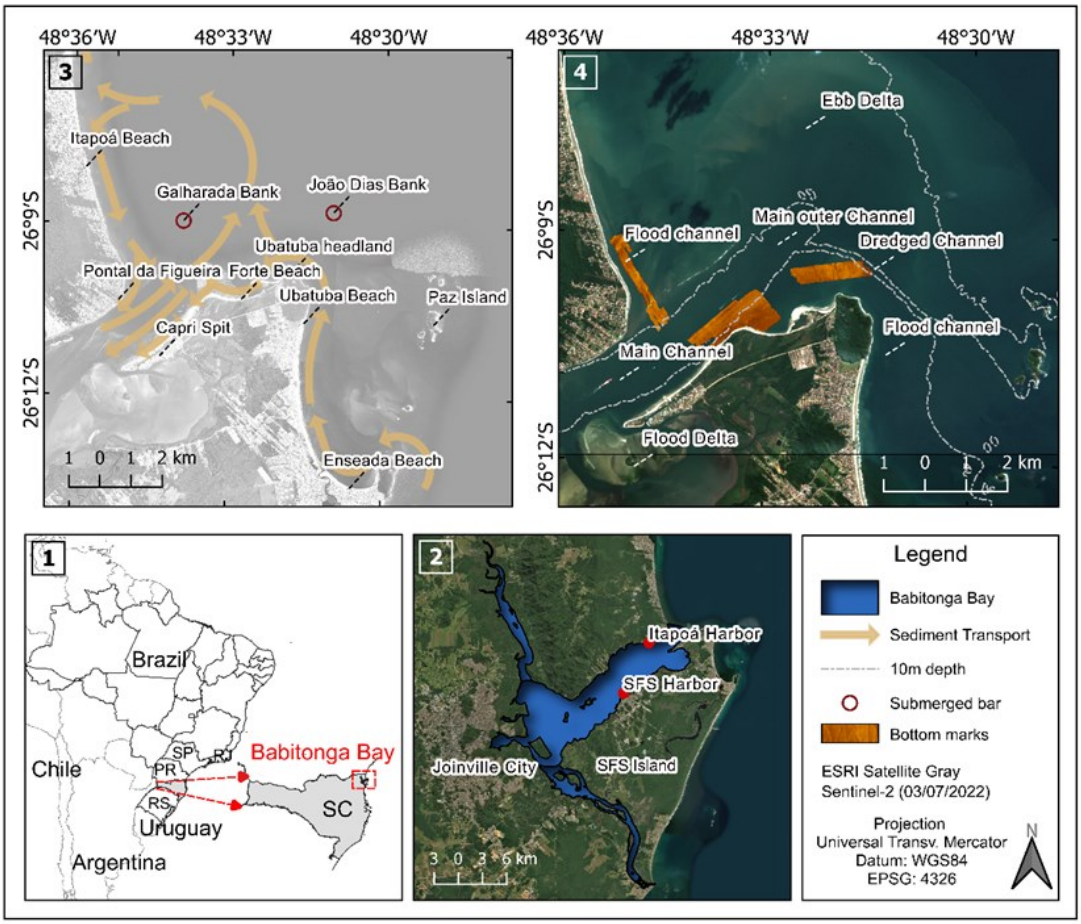

Source: Elaborated by the authors. Basemap from Sentinel 2.

2.3.1 Physical characteristics

The Babitonga Inlet wave climate is dominated by swell from the east (60%), and southeast (27%), while the local waves come from East-Northeast (7%), and Southeast (5%). Average significant wave height is 1.03 m (Alves, 1996), while the mean tidal range is 1.35m (Truccolo; Schettini, 1999). According to the Davis and Hayes (1984) classification, the Babitonga Inlet is a mixed-energy wave-dominated inlet (Fig. 2).

The tidal wave within the Babitonga Bay estuary undergoes substantial transformations as it propagates inland from the mouth. The narrowing of the channel dominates over friction, leading to lateral compression of the tidal wave and an increase in flow velocity. As the tide wave progresses through the 35 km between the inlet and Joinville (Fig.

1), the most amplified constituents are the third-diurnal principal lunar M3 (115%), and the shallow water overtide M4 (82%) (Noernberg; Rodrigo; Luersen, 2020).

Extensive intertidal zones (tidal flats and mangroves) increase the influence of the shallow water constituents, which share the same 3.5 hours oscillation period as Babitonga Bay. This synchronicity leads to resonance phenomena and contributes to the amplification of the shallow water components in the inner regions (Truccolo; Schettini, 1999). The variations in range and phase of specific tide constituents result in ebb flux-dominance. It takes a longer period to flood the bay than to drain it, resulting in an ebb current velocity of 150 cm/s as opposed to a flood flux velocity of 95 cm/s at the mouth during spring conditions (Noernberg; Rodrigo; Luersen, 2020).

Figure 2 - Tidal range and wave height relationships regarding coastal morphology. The yellow square represents Babitonga Inlet.

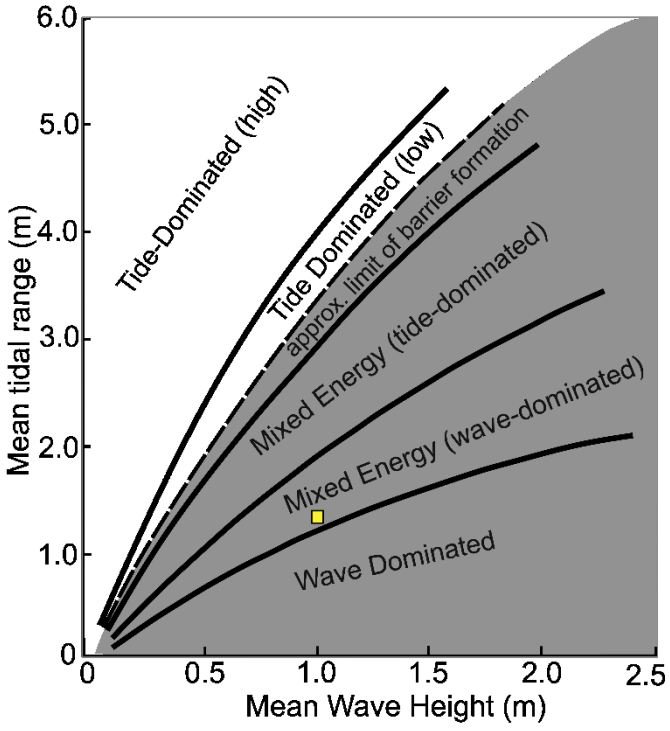

Source: Modified after Davis and Hayes, 1984

2.3.2 Morphological characteristics

The Babitonga Inlet is bounded on the north by a beach ridge plain of Itapoá coastal plain system (Souza; Angulo; Passenda, 2001) and on the south by a headland composed of rocky basement of São Francisco do Sul Island (Cremer, 2006). The main channel is orientated NE-SW and is approximately 5 Kilometers (km) long 3.8 km wide, and has a maximum depth

of 28 m (Vieira *et al*., 2008). The cross-section of the channel is slightly asymmetrical being deeper in the NW (Noernberg; Rodrigo; Luersen, 2020). Inside the bay, the channel has two more elongated portions in the SE-NW direction with a maximum width of 1.5 km and an average depth of 4 m (Vieira *et al*. 2008).

The inlet comprises the following morphological features: outer main ebb channel; marginal flood tidal channels; terminal lobe; and platforms with bars and bed marks (mega and micro undulations) (Fig. 1). The ebb tidal delta is well-developed due to the large tidal prism associated with the 160 km² bay area. The plan shape of the ebb tidal is slightly asymmetrical towards the northeast. because it is protected from S and SE waves in the lee of São Francisco do Sul Island. On the northeast side of the ebb delta, a bar (Galharada shoal) is present on the platform in the shape of a drop, separated from the coast by a marginal flood tidal channel. The northeast limit of the ebb-tidal delta is in front of Itapoá beach.

The inlet sub-environments are maintained by reversing high-velocity currents (>1 m/s). According to Noernberg, Rodrigo and Luersen (2020) during specific time periods, there is concurrent ebb (north side, in front of Itapoá harbor) and flood (south side, in front of Capri Spit) in the 3.8 km-wide inlet. This lateral separation of ebb and flood currents, promotes channel asymmetry through a feedback mechanism that influences morphology, currents, and sediment transport.

The position of the Babitonga tidal inlet is fixed on the southeast side by the rocky headland. The channel is also stable in terms of cross-sectional area, and the shape of the main channel remains relatively constant. Morphological variability is confined to the marginal banks (Capri Spit and Itapoá Beach).

2.3.4 Sedimentary pathways

The Enseada-Ubatuba and Forte-Capri Spit beach systems participate in headland bypassing (Costa *et al*. 2019; Hein *et al*. 2019; Camargo, 2020). Under southerly wave condition sand stored on the headland is transported to Forte beach while easterly waves transport sediment through the Forte Beach-Capri Spit system (Costa *et al*. 2019). The sediment variously promotes extension of Capri Spit, is transported into the flood tidal delta or returning to the ebb tidal delta (Fig. 1) (Silveira *et al*. 2012).

According to the conceptual model proposed by Silveira *et al*. (2012), the sediment that bypasses the headland can take an alternate pathway, instead of being directed toward Forte Beach-Capri spit system, and traverse the southern lobe directly toward the northern lobe. In

areas of the northern lobe where wave effects dominate the tidal flux, cross-shore processes then play a key role in transporting sediment towards Itapoá beach. Upon reaching the beach, the pathway divides into two directions: the portion directed northward gets captured by the longshore current, while the sediment directed southward either nourishes Pontal da Figueira beach or is captured by the flood tidal marginal channel. From the central regions, the ebb tidal flux transports the sediment back to the ebb tidal delta (see Fig. 1).

2.3.5 Human intervention in Babitonga channel

Successive dredging interventions in the ebb tidal delta southern lobe have been deepening the flood channel connecting the former flood channel with the main channel and facilitating access to the harbors of São Francisco do Sul and Itapoá. Initial dredging to 10 m in 1980, was followed by maintenance and deepening operations to reach 14 m depth in 2010 (Fig. 3). The impacts of the dredging activities on inlet bypassing have been previously examined. According to Silveira *et al*. (2012), the dredged channel played a role in deepening the southern lobe of the ebb delta. Firstly, by reducing the volume of sediment that bypasses the inlet via the southern lobe, towards the northern lobe. Secondly, by enhancing the wave energy northward of the channel. Additionally, the decrease in the volume of the northern lobe between 1979 and 1994, as well as the sedimentary deficit of 105 m^3/year along the downdrift coast of Itapoá from 1996 to 2002 was attributed to the removal of sediment that had been trapped within the navigation channel (Angulo; Souza; Lamour, 2006) On the other hand, Pullig *et al*. (2023) attributed the sedimentary loss observed from 1972 to 2021 on both lobes to the weakening of sediment inlet bypassing across the ebb tidal delta. This was attributed to wave climate change and human interventions accelerating a natural starvation period characterized by the end of a wave-dominated stage, that had previously contributed to onshore bar migration.

2.4 MATERIALS AND METHODS

Figure 3 presents the methodology applied to generate Digital Elevation Models representatives of the Babitonga Inlet's terrain over the 1862-1941 period.

Figure 3 - Methodology flowchart

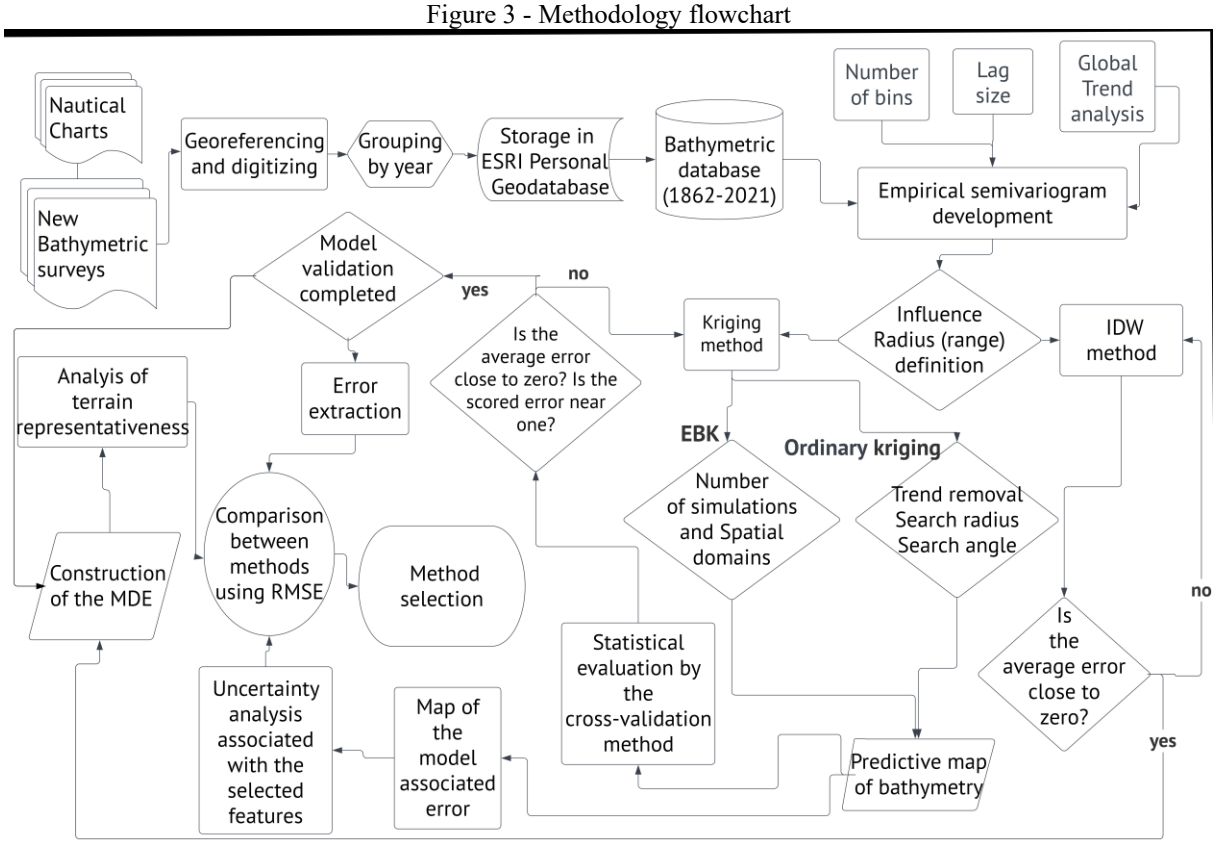

Source: Elaborated by the authors.

2.4.1 Database

This study utilized bathymetric datasets referenced to the mean of the lowest spring tides, extracted from historical charts published by the Brazilian Navy. The nautical charts published in the years 1862, 1941 and 1972 were obtained from the Brazilian Digital Library (Brazil, 2023) while high-resolution copies of the nautical charts published in 1981 and 1995 were provided by the Brazilian Oceanographic Database (BNDO, 2023). A compilation of recent bathymetric datasets, surveyed in 2020 and 2021 years, was also included in the database. The database timeline is presented in Figure 4.

Figure 4 - Timeline of bathymetric datasets (bold) (1862 to 2021) and history of dredging activities in the Babitonga navigation channel (gray) (1980 to 2010). The deepening interventions are displayed downwards, along with the depths they reached, while the maintaining interventions are presented upwards on the timeline.

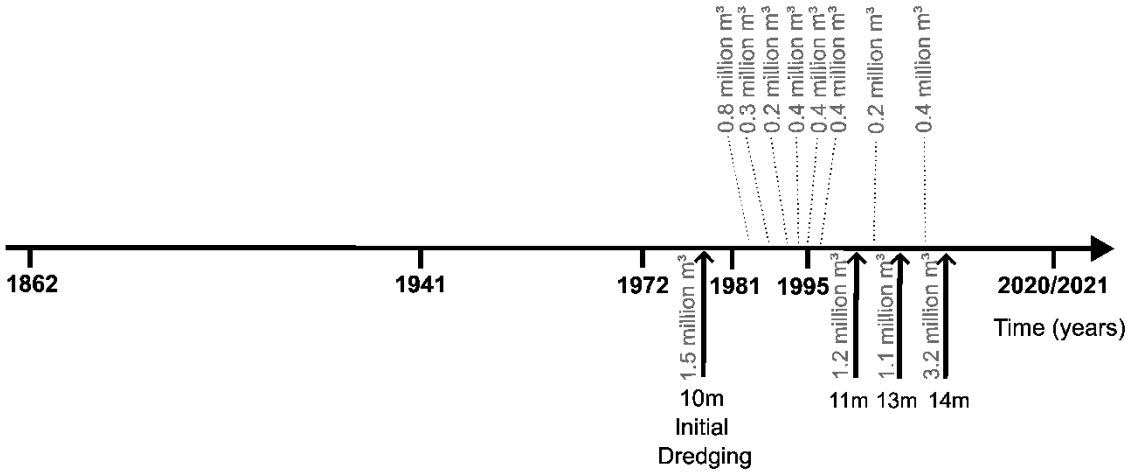

Source: Elaborated by the authors.

2.4.2 Georeferencing and Digitizing

The georeferencing and digitizing steps were performed in a GIS environment. The 1941, 1972, 1981 and 1995 datasets were georeferenced manually with respect to each coordinate system. The 1862 nautical chart was georeferenced using Ground Control Points (GCPs), while the most recent nautical chart of the Brazilian Navy was adopted as the reference layer. The objects used as control points were: the Paz Island lighthouse, the Ubatuba headland peak, rocks and islands in the inner bay, and a crossroad location. Once georeferenced, the documents were stored as GeoTiff files using WGS84 UTM 22S reference system.

The GeoTiff files comprising the bathymetric data were then digitized. The x, y and z coordinate points were assigned to the central position of the numeral to which they referred (International Hydrographic Organization, 2009). Additionally, coastlines, isolines and emerged features contours (tidal bars and islands) were digitized from the nautical chart as polylines. The digitized datasets were recorded in an ESRI Personal Geodatabase.

2.4.3 Data preparation

A histogram analysis was performed on the bathymetric data to identify and correct spurious data resulting from digitization errors. Further, the digitized depths were converted into negative values. The vertices of the coastlines and emerged features (at Mean Low Water) contours were replaced by points, and were ascribed zero depth values.

2.4.4 Exploratory data analysis

2.4.4.1 Trend Analysis

A global trend analysis was conducted using each dataset to select the order of the polynomial function that best fit the data. The direction of the polynomial trend was identifying by rotating the planes perpendicular to the map plane and observing the angle that strongly influenced the polynomial trend.

2.4.4.2 Spatial autocorrelation model

Given the irregular grid spacing of the datasets, the lag size was determined dividing the maximum observed distance among all points by two times the number of bins, while the number of bins was set to 50 (Environmental Systems Research Institute (ESRI), 2021). The lag size, number of bins and trend direction were imputed to develop an empirical semivariogram for each dataset. The mathematical function selected to fit the semivariogram were the one that passed as closely as possible to the binned averaged values and through the center of the binned values cloud. The distance at which binned averaged values presented maximum correlation, and the mathematical model achieved stability, was defined as the dataset range.

2.4.5 Spatial interpolation

A comparative methodology was designed to select the most appropriate method for predict data values in unsampled locations (see. The methodology contrasted the performance of the interpolation methods Inverse Distance Weighting (IDW) (Philip and Watson, 1982; Watson and Philip, 1985), Ordinary Kriging (Matheron, 1971), and Empirical Bayesian Kriging (EBK) (Krivoruchko, 2012). The setting parameters values applied on the selected method (EBK), comparative methodology and performance results are presented as supplementary material in the appendixes.

2.4.6 Raster cell size standardization

The 50X50 m raster cell size was standardized based on the dataset with the lowest sample density. The predictive map obtained from the nautical chart published in 1972 was

converted into rasters at different resolutions (40X40, 50X50, 100X100) to determine which one underwent the least change in converting to raster format.

2.4.7 Performance evaluation

The performance of the interpolation methods was assessed by using cross-validation method (Johnston *et al*., 2001). The analysis among the three interpolation methods relied on the comparison of the Root-Mean-Square Error (RMSE). The performance of the methods was also based on the visual comparison between the isolines (1m, 2m, 3m, 5m, and 10m) extracted from the rasters and the contours extracted from the nautical charts.

2.4.8 DEM comparison

Depth and Slope

The depth and slope changes were assessed through the subtraction of consecutive rasters. The depth change output datasets were in meters while the slope change analysis was carried out assessing the percent rise difference (0-100%). Both map algebra details are given in ARCMAP (2021).

The maps related to the differences in declivity were analyzed joined to the depth difference maps, in order to establish a diagnostic related to the identification of morphological changes on channels and bars. The parameter adopted to assume the appearing of a channel/bar was the identification of an alternate pattern of increasing/flat slope with the flatter region associated to a -1 to -10m vertical loss/2 to 10m vertical gain. The parameters adopted to consider a region as channel deepening/deposit formation were the change occurred in a minimum 0.4km² area. The reasons for that relied on the fact that the regions with minor vertical variations (-1 to 2 m) appeared spread over small areas.

Channel geometry

The 10 m depth contour extracted from the DEMs was assumed as the main channel and outer main channel boundary (Angulo *et al*. 2006) while the 2 m depth contour was used to delimit the Galharada shoal. The Analyzing Moving Boundaries Using R Package (AMBUR package) (Jackson; Alexander; Bush, 2012; Jackson, 2022) was used to evaluate changes in distance between channel boundary and its centerline through time.

2.5 RESULTS

2.5.1 Depth, slope, and geometry historical evolution

The variability in the frequency of the datasets relied on data availability, and addressed the need to deal with different time interval stages along the morphological analysis. Even though the low-resolution of the older datasets comparing to the dataset from 1980 decade, the nautical charts from the 19th and 20th centuries provided a robust foundation for geomorphological evolution reconstruction. After the initial dredging, the Brazilian's Navy bathymetric surveys intensified mostly in the channel, currently used as the navigation channel, while data collection for the northern lobe of the ebb delta has not been published since 1972. Encouragingly, the dataset from 2020/2021 covers the entire study area, including the northern lobe.

To facilitate the analysis at a meso-scale, the results were grouped into the following periods: 1862-1941, 1941-1972, 1970-1990, 1995-2021. Figure 5 shows the simplified bathymetries for full-covered datasets. Figure 6 illustrates the evolution of Babitonga ebb tidal delta and channel between 1862 and 2021 while figure 7 shows the net bed level change for each temporal interval.

2.5.1.1 1862-1941

From 1982 to 1941, the ebb tidal delta changes from a symmetric configuration to an overlapping downdrift lobe. The growth of a predominantly subtidal northern lobe over this 80-year period was accompanied by the formation of an intertidal region (Fig. 5 a,b). The sediment preferentially accumulated in the central part of the northern lobe, closer to the inlet entrance than in the earlier configuration. The formation of interleaved deeper and shallower zones along the seaward sector (fig. 5b) replaced the southeastern main channel alignment from 1862 (Fig. 5a).

Figure 7a show bathymetry and slope change analysis results. A 1.3 km-long sediment accumulation in the middle of the main channel (1 in Fig 7a), is coupled with channel deepening along 2km of both banks on either side of the midchannel accumulation. Bank accretion occurred on both northwest and southeast margins downstream of the midchannel accumulation. The main channel became shallower along 3km due to the formation of several minor deposits in the southeastern side of the channel, measuring 600m, 450m, 700m and 300m-long (respectively 2, 3, 4 and 5 in Fig. 7a). This shallower section is coupled with a 500m width 3km-long deepening of the Northwest bank and a minor deepening on the opposite bank. The results combined suggest that the main channel meandered northwestward associated with

sediment accumulation mainly in the southeastern side of the main channel. Furthermore, the channel deposits morphology's analysis shows U-shaped occurrences, which indicates flood and ebb flow progressively cutting.

In the southern side of the inlet the results show a 1.3-long recurved accumulation attached to Ubatuba Headland (6 in fig. 7a) and a 1.4 km-long bar welded to Ubatuba beach (7 in fig. 7a). In the Northern lobe, in addition to the 1.3-long intertidal linear bar formation, a 2 km-long 1.2-width tailed bar accumulated in northern lobe platform (8 in fig. 7a). Additionally, Figueira beach spit expanded along 3 km up to 1km towards the middle of the channel, while a 3 km-long bar complex attached to the Itapoá coast (9 in fig. 7a).

2.5.1.2 1941-1972

The period is characterized by significant accretion on the ebb tidal delta. Figure 5c shows the coalescence of bars into the intertidal bar. This process increased the downdrift lobe offset and triggered the formation of a 2.7 km length 1.5km width intertidal complex (Galharada). The intertidal complex featured aligned to northeast direction and separated from the Itapoá coast by marginal inflow. The landward sector of the main channel deepens on the northwest side, while on the seaward section the main channel deepens on its southeastern side. The deeper section (between 20 and 29m depth) in channel central sector are filled up and present 8 to 20m depth. The outer main channel shifts its orientation from a northwest towards a north-northwest direction during the period.

Figure 5 - Simplified bathymetry for (a) 1862, (b) 1941, (c) 1972 and d) 2020/2021 datasets showing the cyclic northern lobe asymmetry associated to an outer channel anti-clockwise rotation.

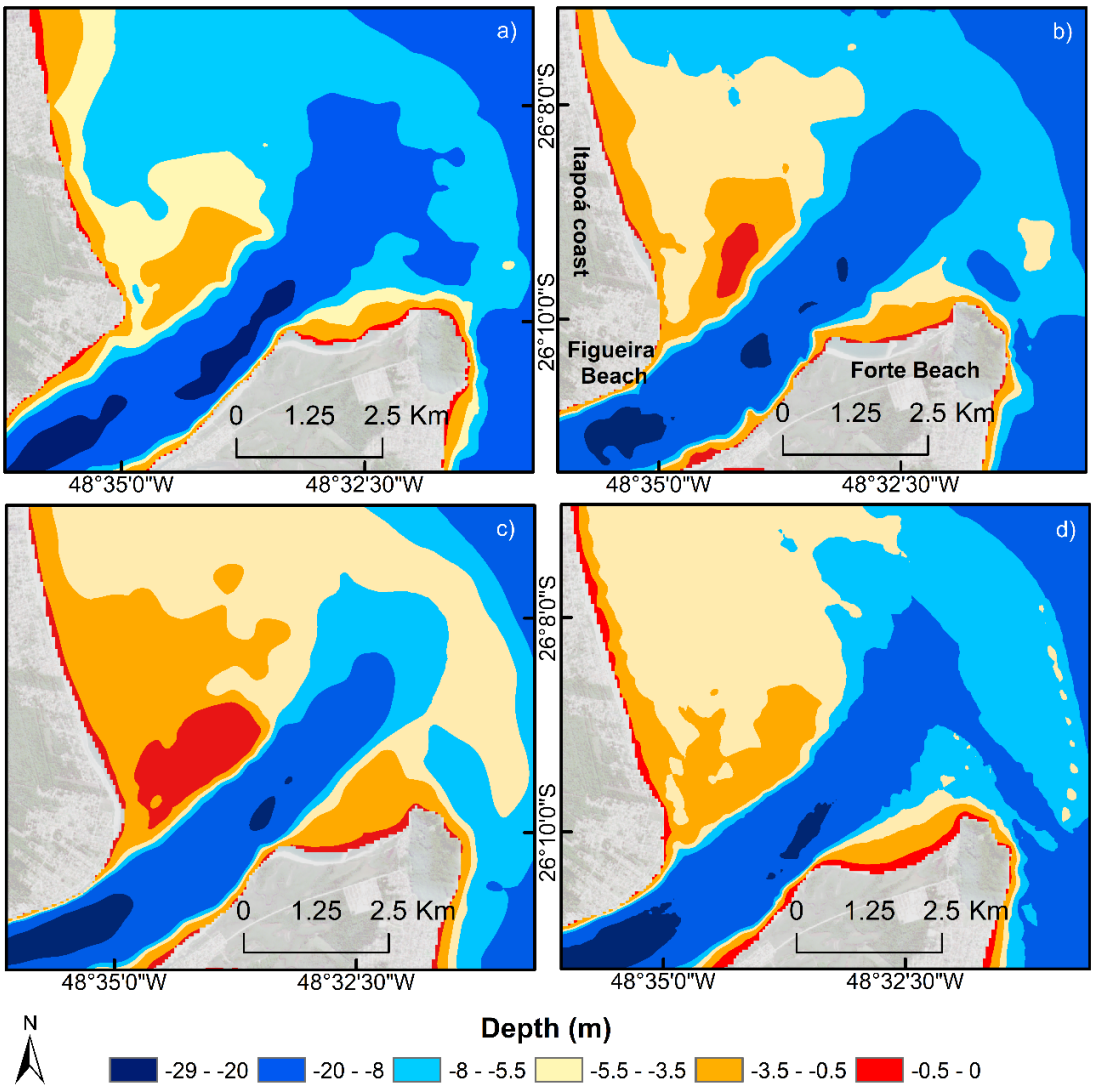

Source: Elaborated by the authors.

The morphological changes from the 1941-1972 period are shown in Figure 7b. During the period the main channel adapted to a new sedimentary pattern as the midchannel deposit were no longer present and significant changes occurred on both banks (see figure 6). At the landward sector, the southeastern bank expanded 700m along 2km (1 in fig. 7b) coupled with the deepening and a 700m retreat of the northwestern bank along 2.3 km (2 in fig.7b). In addition, Figueira beach spit dissociated, suggesting the formation of a straighter, southwest-northeast aligned ebb-dominated channel at the landward sector. At the central and seaward sector, the southeastern bank, Capri Spit, expanded laterally 500m along 2.5km (3 in fig. 7b).

Figure 6: Evolution of the Babitonga inlet: ebb tidal delta and main channel between 1862 and 202.

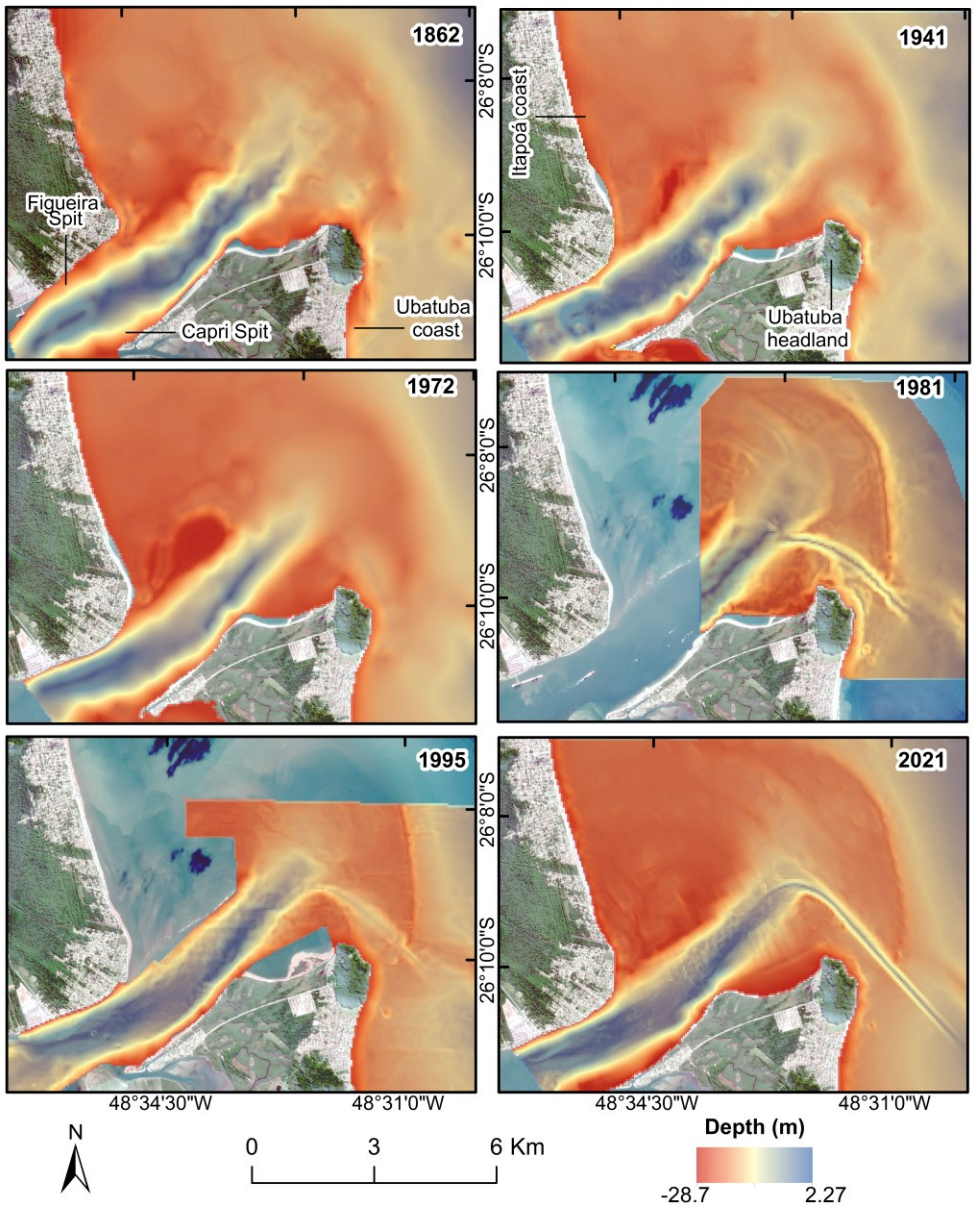

Source: Elaborated by the authors.

The analysis of cross-channel width revealed a decrease in width along the entire length of the channel, in view of the southeast bank expansion. The most substantial reduction, 400m, occurred associated to a midchannel accumulation, pointing that the channel probably curved as the intertidal complex grew, triggering an inner-bend accumulation. The 1.7 km-long 1km maximum width midchannel accumulation (4 in fig. 7b) were coupled with channel deepening along 2km of southwestern bank (5 in fig. 7b). At the southern lobe, the marginal flood channel around the Ubatuba headland meanders northeastward to accommodate a 2km-

long deposit attached to the southeastern bank (6 in fig. 7b) and outer main channel retreats 200m due to the southeastern bank expansion.

Figure 7:Net bathymetric changes for (a) 1862-1941; (b) 1941-1972; (c) 1972-1995 and (d) 1995-2021 temporal intervals, presenting channel northeastward meandering (a), the establishment of a new geometry at the inlet's mouth from 1972 (b), (c) and (d).

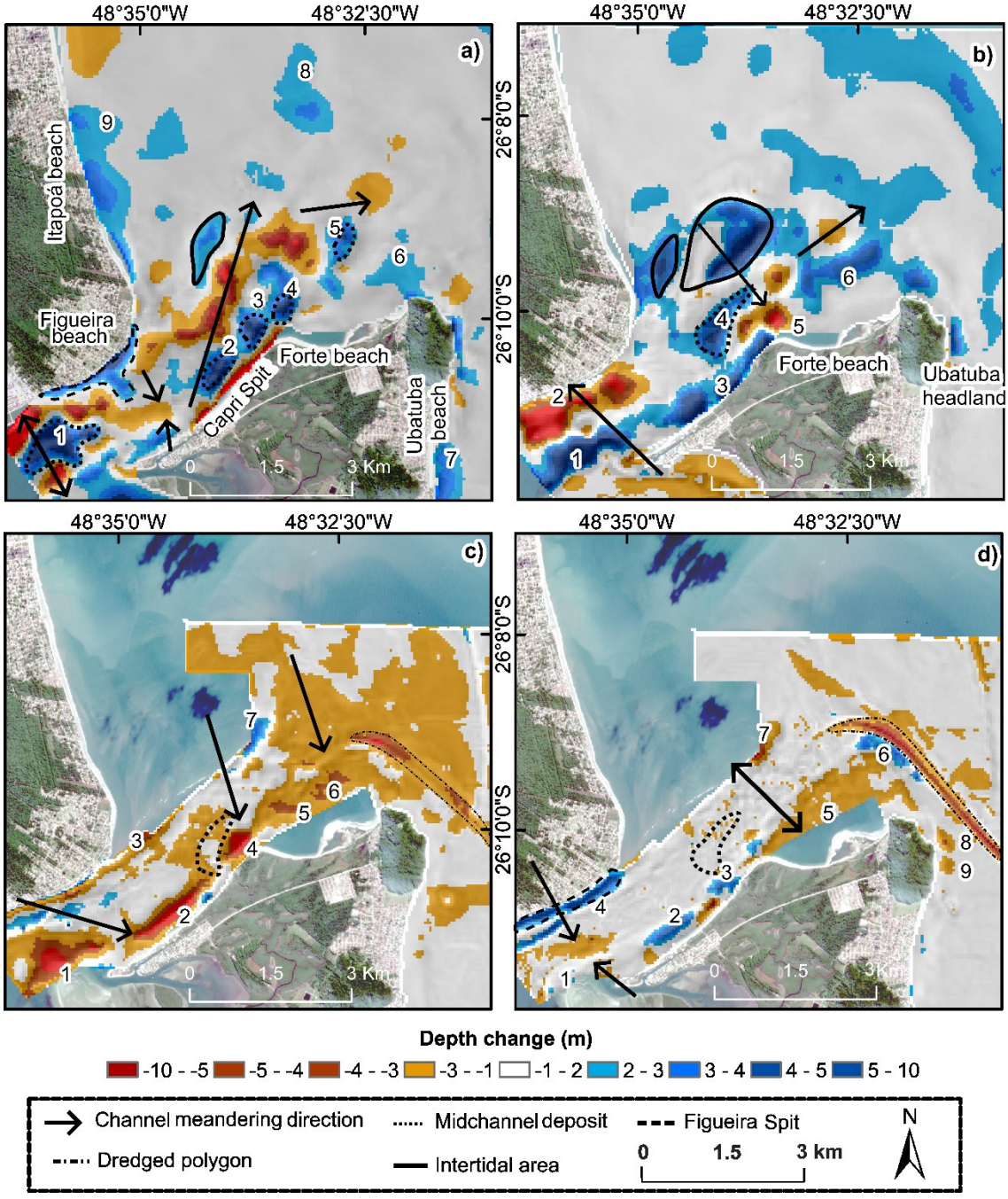

Source: Elaborated by the authors.

The cross-channel width results for 1972 – 1995 period showed channel deepening and 200m channel widening along 1.6km and 2 km at the southeastern bank landward and central sector, respectively (1 and 2 in fig. 7c). Channel deepening continue to occur along 2km on the northwester bank central sector (3 in fig. 7c). The vertical loss at the mouth of the channel expanded 600m landward and extended 500m against the southeastern bank (4 in fig. 7c). Although the channel deepening along the southeast bank, the cross-channel width remained constant along the midchannel deposit accumulated during the last period (1941-1972). This, combined with the southeastern bank scouring at the mouth, and the persistence of the midchannel deposit, indicates the channel continued to bend while the outer main channel orient toward north-northeast direction and sediment accumulated in the middle of the channel at the mouth. Moreover, Galharada linear bar expanded 280m seaward (7 in fig. 7c).

Figure 8 shows the depth changes in a decadal scale during the 1972-1995 period by incorporating the 1981 dataset. It can be noted that the vertical loss throughout the ebb tidal delta, as seen in Figure 8c, primarily occurred between 1972 and 1981 (fig. 8a). Between 1981 and 1995, sediment loss was observed only on the southeast side of the outer main channel in the southern lobe (fig. 8b).

From 1970 to 1980 across- channel- oriented sediment points within the main outer channel, from the southeastern bank to the northern lobe, measuring 250m in length and 400m in width and presenting a vertical accretion of 2m to 6m. Furthermore, during this period, the Galharada bar retreated 150m at its southeastern boundary. The dredging signature in figure 8a was associated to the initial deepening of the shipping channel in the ebb delta southern lobe. This intervention connected the flood channel in the southern lobe to the main ebb channel in the ebb tidal delta in 1980. At the southern lobe, the southeastern bank retreated 150m, probably associated to the establishment of a secondary flood channel southward of the former flood channel (fig. 8a)

From 1980 to 1995, the results show the absence of the vertical accretion points within the main outer channel and sediment accumulation around the headland, within the secondary flood channel. Galharada bar extended laterally up to 150m southeastward (thus returning to its position in 1972) and expanded 280m seaward. This result suggests two distinct phases in the sedimentary bypassing across the ebb tidal delta. Initially, the channel around the headland dominates, transporting sediment to the main channel mouth. Subsequently, when the flood channel fails to deliver sediment to the inlet entrance, and it accumulates around the headland, the sediment is instead transported through the terminal lobe pathway.

Figure 8:Net bathymetric changes over a) 1972-1981, indicating a sedimentary bypassing across the ebb tidal delta, and b) 1981-1995, the seaward expansion of Galharada linear bar.

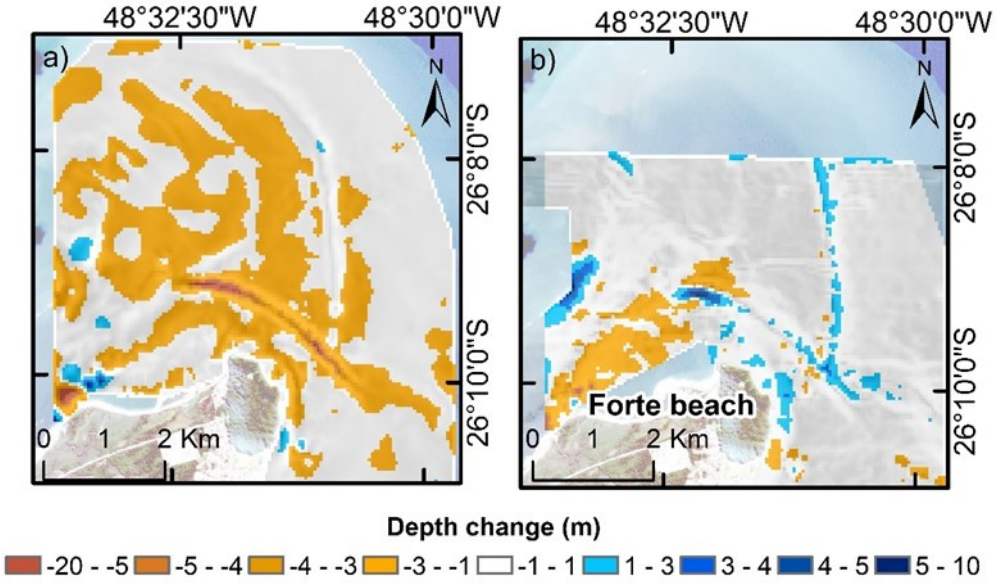

Source: Elaborated by the authors.

2.5.1.3 1995-2021

The 1995 – 2021 period have been marked by sediment retention along both banks on the landward and central sectors (Fig. 7d). The southeastern bank (Capri Spit) extended 150m, 200m and 100m at 3 locations along 4 km (1, 2 and 3 in fig. 7d). Conversely, Figueira beach spit on the northwestern bank extended 150m along 2.5 km (4 in fig. 7d). At the region where the midchannel deposit is located, the cross-channel width remained unchanged since 1972. However, the outer main channel experienced an average increase in width of 200 meters.

In the ebb tidal delta, the results showed the deepening of the outer main channel along 2km of the southeastern bank (5 in fig. 7d), scouring the southern lobe. Dredging activities deepened the shipping channel to 14m depth in 2010 and the dredging polygon was redrawn toward north while a 1.5 km-long region aligned parallel to the shipping channel presented vertical accretion of up to 5 meters (6 in fig. 7d).

Since the 1995 dataset lack of data at the entire northern lobe, it was only possible to state that the Galharada bar retreated 700m from 1995 to 2021 (7 in fig. 7d). Nevertheless, the dataset from 2021 was compared to the 1972 dataset to better understand the changes across the northern lobe. The results indicate the replacement of intertidal areas, that had reached their apex in 1972, by a linear bar with a minimum depth of 1m cutting through two marginal channels (see figure 6).

The results also revealed 400m and 200m-long regions around the Ubatuba headland, experiencing vertical losses of up to 4m (8 and 9 in fig. 7d). The accumulation along the southeastern main channel bank coupled with sediment liberation around the headland suggests sedimentary transport toward the channel over the period

2.6 DISCUSSION

2.6.1 Morphological Evolution

Channel confluence and divergence

During the first 80 years of analysis (1862 - 1941) the establishment of isolated deposits at the estuary entrance played a key role in channel geometry. The channel experienced the development of confluence and divergence zones, resulting in an increased meandering and quasiperiodic width variation in channel planform (See figure 5a and figure 6).

The formation of isolated deposits in the middle of the channel should be associated to divergence zones formation. Downstream of the midchannel deposit, Capri Spit extended laterally, as well the Figueira spit, deflecting the flow toward the middle of the channel, creating a potentially erosional confluence zone (Leuven, 2019). This configuration likely caused the flow to converge in the cross-channel direction. As the outflow move sideways from the midchannel deposits isolated at the inlet's entrance and approaches the ocean side, it impinges against both banks. Along the southeastern bank, the flow is likely captured by the marginal channel, preventing the isolated deposits to attach to Capri Spit. Consequently, sediment bypassing the headland, coming from Ubatuba beach, tends to accumulate in the middle of the channel, at the inlet's mouth. Along the northwestern bank, the outflow deflection encounters less resistance due to the absence of rocky substrate, favoring lateral scouring. Therefore, the channel migrates northeastward.

The outflux defection toward northwest likely contributes to the transport of sediment from the Galharada bar to the Itapoá coast. The ebb tidal currents now directed toward the bar carry the sediment put in motion by wave breaking during intertidal exposure, subsequently depositing it on the beach. Due to the low temporal resolution of bathymetric data over the first 80 years, we cannot definitively state, but given the length of the period, it is likely that the intertidal area of Galharada underwent cycles of expansion and erosion as it eroded by the

deflection of the ebb flow towards the northwest, and grow due to wave-built swash bars coalescence, left behind the intertidal contour that is observed in the 1941 dataset (see fig 5b).

Sediment transport from Itapoá beach could have contributed to the Figueira spit growth and midchannel accumulation. The sediment transport in Babitonga Bay is influenced by a recirculating cell in the northern lobe, which redirects sediment from Itapoá towards the channel (Silveira *et al*., 2012). Hence, one may anticipate that the bar attached to the downdrift coast played a crucial role in providing sediment into the channel, leading to the creation of convergence and divergence zones. This process likely established a morphodynamic feedback that ensured the establishments of the bars attached to Itapoá coast.

Meanwhile, the channel cutting process observed in the midchannel deposits should have occurred due ebb and flood flux increase. As the flow scours the banks and supply sediment to the midchannel deposits, the increasingly slope amplified both ebb and flood currents (Leuven, 2019). This process commonly results in deposit dissociation.

2.6.1.1 Ebb tidal delta sand trapping

During the following period (1941 – 1972), a reduction in channel meandering can be a consequence of the ebb flow constriction in the along-channel direction. The amplified ebb and flood flow due to current-slope interaction favored the establishment of an ebb-dominated main channel in the landward and central sectors, while the marginal channels became flood-dominated. As the southeastern bank expanded, the latter acted as a bridge, facilitating the transport of the sediment accumulated at the downdrift-headland compartment (southeastern bank in the ebb tidal delta) toward the landward sector. Therefore, the southeastern bank expansion constricted the ebb flux against the northwestern bank. This is likely associated with the establishment of a residual ebb flow mainly on the deepest northwest margin (Noernberg; Rodrigo; Luersen, 2020). Due to the hypersynchronicity of Babitonga Bay, ebb currents are stronger and thus have a greater scouring capacity. Therefore, the establishment of an ebb-dominated channel in the Babitonga Inlet is associated to an asymmetry in cross-sectional depth, mainly because of the headland bypassing supply. Additionally, the variation in cross sectional area along the channel probably increased the flow velocities. This phenomenon can be attributed to the change in channel geometry at the landward sector as a result of lateral constriction (Speer; Aubrey, 1985).

The development of the Galharada complex should have been a result of swash bar formation in the terminal lobe region, combined with landward migration and coalescence

(Fitzgerald; Kraus; Hands, 2000). As the Galharada complex expanded, one would expect an increase in wave refraction and diffraction around the northern lobe of the ebb tidal delta. This wave transformation could have facilitated the trapping of sediment from longshore transport due to current reversal along the downdrift shoreline (FitzGerald, 1984). Moreover, variations in the direction and strength of the longshore current have been associated to wave climate change (Trombetta *et al*. 2020). This suggest that the process of refraction, combined with wave climate change, favored the expansion of Galharada despite its intertidal exposure, and weakened the sediment transport towards the Itapoá coast.

2.6.1.2 Channel realignment

The growth of Galharada, associate to the dominance of secondary flow, could have constricted the channel's mouth against the updrift shoreline during the 1941 – 1972 period. The growth of Galharada favored the transverse circulation along the flow direction (Aubrey; Speer, 1984; Elias; Van Der Spek, 2006). The channel curves leading to a reduction in bottom flow along the channel. This imbalance is resolved by redirecting the bottom flow towards the inner part of the curve. This process may have triggered the accumulation of an inner-bend midchannel deposit at the mouth. Similarly, the difference between water depth average and surficial flow resulted in outward flux, impinging the flow against the updrift bank (Elston, 2005).

During the decade of 1972-1981, the Babitonga Inlet underwent significant transformations, attributed to the establishment of this new geometry at the inlet's mouth and the cross-sectional asymmetry. Firstly, the deepening of a new flood channel southward of the former flood channel, around the headland, initiated the deepening of the southeastern bank in the ebb tidal delta. Secondly, the outer main channel orientated toward northward. This new flood channel around the headland began to transport sediment previously trapped at the southeastern bank in the ebb tidal delta (see fig. 8a), shifting the dynamics of inlet bypassing. These changes likely involved the redistribution across the ebb tidal delta of the sediment supplied by the headland bypassing process.

In the years following (1981-1995), the observed asymmetry along the outer channel suggests a deepening along outer channel the southeastern side, strongly favoring the connection between the channel and the ebb tidal delta through its southern lobe. Concurrently, the expansion of Galharada seaward indicates that the sediment previously trapped within the

channel (see fig 8) has reached the northern lobe, and now is redirecting the outflow towards southeast.

The growth of Galharada bar complex may have resulted in the division of the ebb tidal delta into two sub environments. As Galharada grows seaward and secondary flow eroded the inlet's mouth outer bank (Aubrey; Speers, 1984), one may expect the favoring of the connection between the channel and the southern lobe, potentially eroding the southern lobe and isolating the northern lobe, as described by Elias; Van Der Spek (2006) to the Texel Inlet. This preferential connection, favored by the dredging since 1980, may have impeded the channel to complete the inlet bypassing cycle and return to its configuration in 1941 (see figure 6).

2.6.1.3 Bypassing pathways in a decadal scale

The absence of evidence of sediment transport along Enseada-Ubatuba and Forte beach-Capri spit beach systems during 1972-1995 period (see fig. 7c) indicate the weakening of the headland bypassing pathway, mechanism that pushes sediment from the updrift portion of the headland toward the channel, as described by Costa *et al*. (2019). Nevertheless, the sediment deposits across the outer channel and Galharada seaward expansion over the same period suggest a temporary mechanism of inlet bypassing across the ebb tidal delta (see Fig. 7). Moreover, it indicates that the longshore current direction returned to north. Even though the evidences of sediment transport along the terminal lobe from 1981 to 1995 imply a sedimentary pathway dominated by wave-induced transport, the absence of swash bars formation strengthens the hypothesis that inlet bypassing in a decadal scale is dominated by an across-ebb tidal delta pathway through a minor shift in the outer main channel alignment, rather than swash bar formation and landward displacement (Fitzgerald, 1982; Fitzgerald; Kraus; Hands, 2000).

2.6.1.4 Inlet response to dredging interventions

Previous studies have examined the link between dredging and the extent of sediment bypassing in the Babitonga inlet (Angulo; Souza; Lamour, 2006; Silveira *et al*. 2012; Brazil, 2019). The shift of the former flood channel into a narrower and deeper shipping waterway resulted in a convergence of width (see fig 6c). The modification is likely to have amplified the amplitude of the tidal wave and increased the velocity of the tidal currents, generating a funneling effect on the flow (Jay; Leffler; Degens, 2011; Ralston *et al*. 2018; Familkhalili; Talke, 2016), as they shifted the equilibrium between convergence and friction effects on tidal wave propagation (Friedrichs; Aubrey, 1994). Thus, one may expect the dredging extended the

reach of the ebb flux seaward by establishing a preferential connection between the main ebb channel and the deeper section of the delta. This preferential connection may have triggered the formation of a new marginal channel, considering that in the Babitonga Bay estuarine circulation occurs laterally (Noernberg; Rodrigo; Luersen, 2020).

From 1995, the inlet changed significantly. Particularly, the deepening of the southern lobe (see fig 7d), and the evidence of sedimentary connection between Ubatuba beach and Capri spit. The changes could be consequence of a shift on sedimentary processes at the entrance of the estuary. First, the difference in depth between the dredged channel and the surrounding area should have addressed variations in wave propagation velocity inside and outside the channel, resulting in phase difference. When waves approach the channel with a slightly oblique angle, they refract just enough to remain on the channel slope, increasing wave height and concentrating wave energy along the channel, until they become unstable. The instability cause waves to change their course and move sideway from the channel. Therefore, the wave energy, that was originally dispersed across the ebb delta, might now be influenced by the navigation channel, which is actively transporting sediment laterally (Zwamborn; Grieve, 1974). This phenomenon could be enhancing the impact of more energetic waves, likely originating from the south/southeast quadrant (Alves, 1996), in account of the incoming wave angle. Moreover, the erosion observed in the seaward portion of the ebb delta, northward of the dredged polygon, especially prominent since 1995, aligns with the outcomes of Silveira *et al*. (2012) model, which suggests an increase in wave energy to the north of the dredged channel 10 years after the initial dredging. Second, after 1995, the deepening interventions could have favored the sediment transport through headland bypassing mechanism, coinciding with erosion observed across most of the ebb tidal delta.

This hypothesis suggests that the dredged channel is potentially acting as a hydraulic barrier to the longshore flux. Thus, the sediment transport into the channel is favored, thereby facilitating Inlet bypassing through tidal currents via the channel and weakening sediment transport across the ebb tidal delta, toward the northern lobe. Additionally, the Silveira *et al*. (2012) model also anticipated a reduction in mean energy flux southwest of the dredged channel. This reduction may contribute to accumulate the sediment bypassing the Ubatuba headland until favorable wave conditions redirect it into the channel.

2.6.1.5 Ebb tidal delta asymmetry

The results point an increasing of the ebb tidal delta northern lobe offset over the first 110 years (1862-1972). During the period, the bar attachment to the Itapoá coast and the subsequent growth of the intertidal Galharada complex contributed to the shift from a symmetrical ebb tidal delta to a northern lobe overlapping (see Figure 5 and 6). From 1972 to 2021, the ebb tidal delta developed symmetrically. The shift in the alignment of the ebb tidal delta offset seems to be associated to the stability of the inlet's mouth geometry, especially since 1995.

In addition to the geometric stability at the inlet's mouth, two reasons could prevent the ebb tidal delta asymmetry from that point forward. First, as the ebb flow created new seaward connections, this could have triggered the swash platform to displace seaward in the southeast direction, which would increase the time required for sediment to reach the downdrift portion through wave-induced transport. Second, the sediment that would accumulate in the southern lobe may be redirecting into the channel, due to the deepening of the ebb tidal delta and flood flow-dominance along the headland vicinity.

2.6.2 Conceptual model of headland-controlled Inlet bypassing

In an updrift headland-controlled inlet, as occurs in Babitonga, the constraining effects of the back barrier steering (Elias; Van Der Spek, 2006) play an even more decisive role in the evolution of the ebb tidal delta and adjacent coastlines. The basin-channel orientation constrains the outflow configuration onto the ebb tidal delta and affect the headland bypassing mechanism, that may or may not result in a pathway for longshore sediment transport. On the other hand, the headland impacts on the development of a southern lobe by realigning the ebb jet on the ebb tidal delta and sheltering inlet's portions.

The conceptual model presented in Figure 9 addresses the natural morphological evolution of a headland-controlled meso-scale mixed-energy inlet, regarding long-term shifts on sedimentary pathways of associated headland-Inlet bypassing. The description provided below expands upon concepts from Oertel (1975), Short; Masselink (1999), FitzGerald (1984), Fitzgerald, Kraus e Hands (2000), and Elias; Van Der Spek (2006) and uses the 'flow-deflection zone' referring to the region dominated by headland-induced wave effects due to tidal flow deflection.

Figure 9:Conceptual model for associated headland-inlet bypassing accounting of Inlet's configuration presenting (a) the channel capturing the alongshore transport; (b) ebb tidal delta sand trapping, and (c) alongshore transport-dominance.

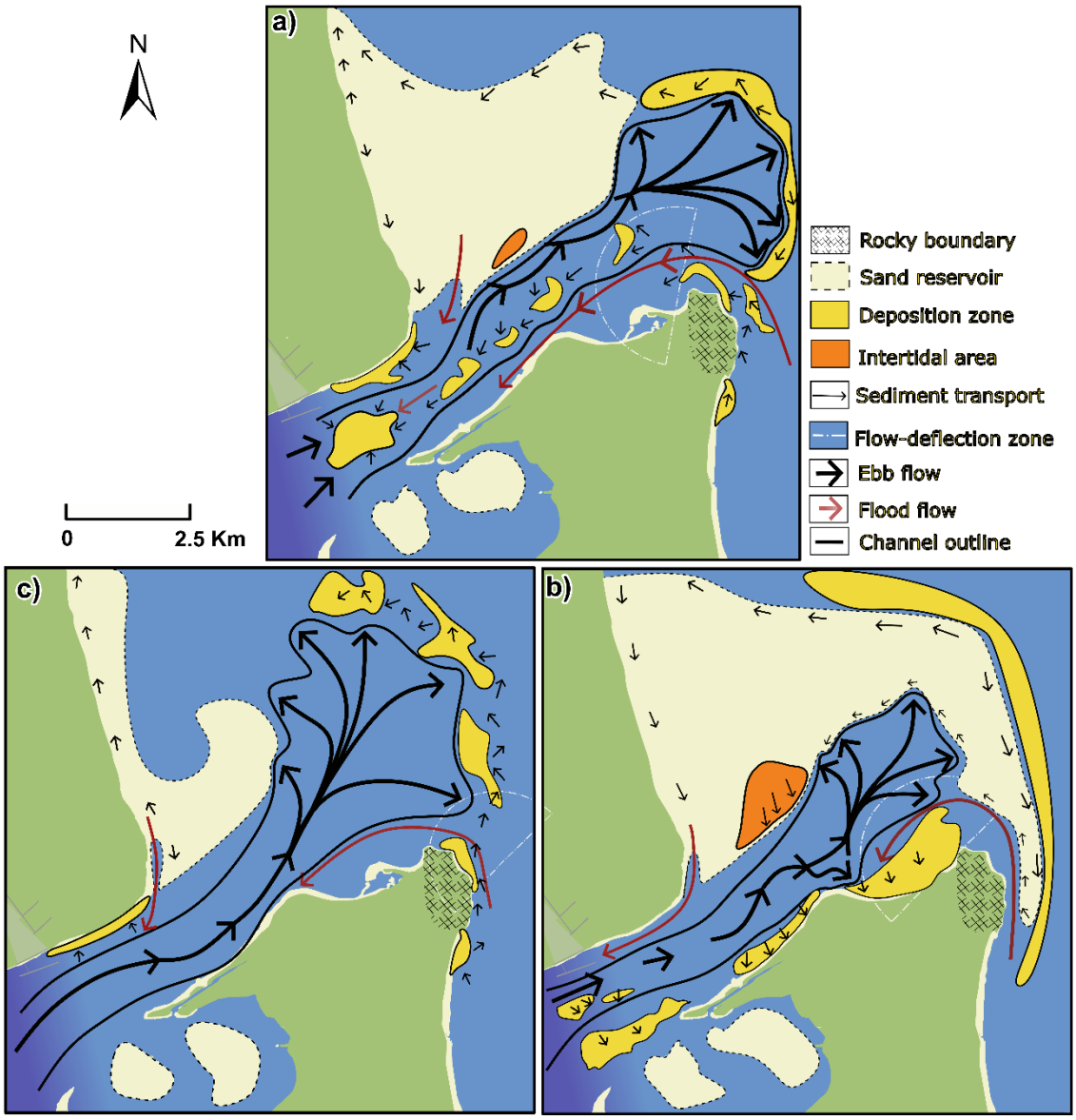

Source: Elaborated by the authors.

Considering a deep channel tidal inlet comprising a well-developed ebb tidal delta and constrained by an updrift headland-induced offset. Waves tend to approach nearly perpendicular to the north face of the headland, due to refraction. The enhanced bed shear stress influences the tidal flow that avoids wave-dominated directions. Consequently, the sand wave that moves around the headland toward the downdrift compartment is prevented from being transported seaward during ebb flow, while during flood flow it experiences a landward-directed transport. If the balance between wave energy and tidal current favors a greater

penetration of wave force, the 'flow-deflection zone' displaces landward, and the sand wave moves around the headland toward the channel, shaped as an elongated spit. Meanwhile, the tidal flow onto the ebb tidal delta become increasingly downdrift orientated. At that point the direction of the boundary-headland rip coincides with the direction of the residual transport along the immediately downdrift compartment. Hence, the direction of residual transport along the compartment immediately downdrift of the headland is toward the basin-channel (Fig. 9a).

While the inlet's mouth is downdrift aligned, the flood flow dominance immediately downdrift from the headland plays a key role in preventing the migration of the sand body across the ebb tidal delta. In the headland bypassing model described by Short and Masselink (1999), the submerged spit migrates along the coast subaqueously, merging with the downdrift shoreline. In the proposed model, sand bypassing the headland is transported by the flood flow and settles along the southern side of the channel-basin due to opposing tidal currents. Near the flood tidal delta, the flood flow loses velocity, ending the transport of sediment captured from longshore transport. Consequently, the updrift side of the basin-channel gradually becomes shallower, and the channel widens primarily at its landward portion, narrowing the channel sector downstream of the midchannel deposit. While the accretion on the channel-basin is constrained by the outflux/influx in the channel, the cross-channel asymmetry induces the channel (and so the outer channel) to meander toward the downdrift bank. Therefore, the accommodation of sand along the channel-basin is addressed by the erodibility of the downdrift seabed and the rate of expansion of the northern lobe (fig. 9a).

The formation of the midchannel deposits and cross-sectional asymmetry in the along-channel direction has significant implications for the Inlet morphological evolution. The narrow channel sections become constricted and the ebb flow accelerates into the ebb tidal delta (Oertel, 1975). This constrains the flow at the inlet's mouth toward an increasingly downdrift orientation. Furthermore, the outflow acceleration increases its capacity to transport sediment seaward (Oertel, 1975), allowing the ebb tidal delta to expand beyond the headland constriction and shape toward a free-form (Hicks and Hume, 1996). As a result, the ebb tidal delta expansion occurs aligned with the outflow downdrift direction in the inlet's mouth. This shift leads to an ebb tidal delta morphology that resembles that of a tide-dominated inlet described by Hayes (1979).

Furthermore, at the downdrift inlet shoreline, the outflow acceleration enhances the ebb jets as well as the tidal residual transport across the downdrift lobe. The intensification of the recirculation cell amplifies the role of the ebb tidal delta's downdrift portion in reserving

sediment from longshore transport, creating a sediment transport gradient to the south (FitzGerald, 1984). The growth of the flood tidal delta also contributes to a well-developed residual circulation inside the inlet, favoring the formation of a spit. The southward residual transport leads the linear bar to growth into an intertidal complex, by influencing the direction of the swash bars migration, while a updrift-directed spit-barrier develops (Fig. 9b).

As the outer main channel become increasingly constricted by the northern lobe expansion, terminal lobe, the outflow accelerates and the terminal lobes expands by approximately one-third of the inlet's mouth width. Meanwhile, as the spit-barrier continues to grow updrift-directed, it influences the seaward protrusion of the outer main channel, causing it to retract by two-thirds of the inlet's mouth width, but increases its length alongshore, since it tends to flow parallel to the spit. Consequently, the outflow onto the ebb tidal delta become oriented in a manner that ultimately led to a hydraulic inefficiency. Hence, the outflow breaches the ebb tidal delta seeking for a more efficient configuration inducing the formation of an updrift-directed outer main channel branch.

The southern branch formation shifts the flow-deflection zone seaward, as it increases the dominance of outflow at the region sheltered by the headland. This inaugurates a new wave-tide balance that induces a longshore sedimentary pathway. The sediment migrating around the headland (Short; Masselink, 1999) is now displaced seaward of the surf-zone and transported through the ebb shoals, near the closure depth, continuing to migrate driven by wave-induced longshore transport (Fig. 9c) (Ab Razak, 2015; Fitzgerald; Kraus; Hands, 2000).

The research on the morphological evolution of Babitonga Inlet provides evidence of headland bypassing process influences on the development of an ebb tidal delta southern lobe in a rocky boundary-inlet dominated. As the sediment is redirected toward the channel due to headland-bypassing, creating narrow and widen cross section and enhancing channel scouring, the sediment is pushed mainly toward the flanks of the outer main channel in the northern lobe, inducing sediment starvation in coastal portions further downdrift from the inlet entrance (see fig. 5b, fig. 6 and fig. 9a). This occurs accounting of the shelter provided by the headland at the southern lobe, that prevents sand distribution across the swash platform and along the terminal lobe. The associated headland-inlet bypassing process, thus, favor southward transport along the downdrift shoreline, which can induce longshore reverse transport (fig. 9b). Moreover, the findings align with those from Costa *et al*. (2019) regarding the influence of tidal flow on headland bypassing along the Babitonga Inlet coast. Their work identified a synergistic effect

of tidal currents and waves in transporting sediment toward the southeastern bank (Capri Spit), as one may expect the southern lobe dominated by tidal currents.

Conversely, the prevalence of the longshore pathway due to channel southern branch formation occurs simultaneously to the overlapping of regions further downdrift from the inlet's entrance (see fig. 5a and fig. 9c). This finding suggests that specific inlet configuration may be necessary for sediment to reach regions farther beyond the downdrift ebb tidal delta circulation cell on a headland-controlled inlet. Furthermore, the orientation of the ebb channel towards an updrift direction has been described as likely to strengthen the wave-induced sediment bypassing along the terminal lobe of the ebb tidal delta (Lenstra *et al*. 2019). Thus, the alignment of the outflow in an updrift direction could also have induced the longshore sedimentary pathway.

2.6.3 Comparison with previous conceptual models

The rocky headland control on the updrift side of a meso-scale estuary, as seen in the Babitonga Inlet, results in bypassing mechanisms that differ from those described earlier. The preferential deposition of sediment has been described limited to the updrift portion of the ebb tidal delta and shifts in channel alignment have been associated to cyclic ebb tidal delta breaching mechanism (Fitzgerald 1982, 1988; FitzGerald; Kraus; Hands, 2000; Elias; Van der Spek, 2006). At the Babitonga Inlet, the sediment accumulation updrift of the inlet is not restricted to the ebb tidal delta, but extends into the channel-basin due to headland bypassing-associated sand bridge. In addition to the influence of headland bypassing mechanism, the ebb flow is unable to remove sediment from the channel flanks in the southern portion of the main channel, since it is dominated by flood flow. The flood currents tend to push sediment into the channel, directing it toward the headland-beach, Capri spit, and the flood tidal delta, continuing to fill the southern marginal compartments until the channel reach a new configuration.

The annual process-based conceptual model proposed by Silveira *et al*. (2012) states that the sand bypassing the Ubatuba headland might take the Forte Beach-Capri spit system as a pathway to the inner bay, or directly reach the northern lobe of the ebb tidal delta. The meso-scale model proposed in here suggests that the lateral expansion due to sand accumulation along the Capri-Spit can change the channel and shoal dynamic of the Babitonga inlet. The lateral growth of Capri-spit constrict the opposite section of the main ebb channel against the northwest shoreline, Figueira Beach-spit. The results suggests that this process eventually lead this landward section to deepen and redistribute sediment along the downdrift channel sections and

ebb tidal delta compartments. Depending on the major deposition zone, the ebb tidal delta can change significantly, even triggering a reverse longshore transport along the inlet-dominated coastal portion.

The model for Inlet evolution proposed here contrasts with that based on the Oregon Inlet evolution. In the model elaborated by Velasquez-Montoya, Overton e Sciaudone (2020) the outflow rotates toward an updrift orientation onto the ebb tidal delta, and the flood shoals on the channel-basin tend to deviate from the along-channel direction. In Babitonga Inlet, as the outflow experience an updrift rotation the flood shoals migrate to the southern portion of the channel-basin allowing the flood tidal delta to growth and force laterally the channel. The sand spit extension along the southern bank, combined with the flood tidal delta expansion, push the channel-basin northward, while the ebb shoal growth constrains the inlet's throat southward.

The concept on the development and attachment of the bar complex based on Price Inlet by FitzGerald (1984) describes a stage of transport reversal induced by waves refracting around the bars along the adjacent shoreline, trapping a large amount of sand entering the inlet. Although the Babitonga Inlet exhibited a period in which the morphological characteristics are compatible with this stage, it is reasonable to consider the hypothesis that the trapping may have been favored by the sediment supply from the coarser sediment regions within the estuary itself. In the model of transport for irregularly shaped estuaries, the asymmetry of tidal currents is mainly influenced by the estuary's geometry (Dronkers, 1986). The growth of the flood delta due to the establishment of the headland-associated sand bridge toward the channel increased the intertidal area above mean sea level and influenced channel depth, inducing maximum ebb currents that facilitate the seaward flux of coarse suspended sediment, ultimately increasing sand supply for the ebb tidal delta.

2.7 CONCLUSION

A compilation of bathymetric datasets surveyed along the Babitonga Inlet over 160 years results in a long-term morphological database (1862-1941). A conceptual model is proposed addressing the natural morphological evolution of the rock-controlled Babitonga Inlet. The model describes the initial stage as characterized by a downdrift basin-channel orientation, in which nearshore headland bypassing and residual transport towards the channel-basin results in the formation of narrowing and widen sections along the channel, accelerating

the outflow onto the ebb tidal delta and inducing a longshore transport reversal on the downdrift lobe. During the next stage, the growth of an intertidal complex constricted the outflow against the updrift shoreline and ebb flow is redirected toward the southern lobe due to the formation of an updrift-oriented branch. The channel realignment induces the seaward distribution of sediment that bypasses the headland, supplying a wave-induced longshore sedimentary pathway through the ebb tidal delta outer shoals.

Future work should employ process-based long-term modelling addressing headland-controlled inlets morphodynamic to assess the contribution of morphological changes. Furthermore, it is crucial to consider the increasing frequency of storm surges and changes in wave climate in future studies addressing inlet evolution.

2.7 DATA AVAILABILITY

The Digital Elevation Models (raster format) generated from the bathymetric datasets are available in https://data.mendeley.com/datasets/v2gp34d6rt/1.

2.8 ACKNOWLEDGEMENTS

We would like to thank the National Council for Scientific and Technological Development CNPq-Brazil (project RiscPorts No. 441545/2017-3) for providing the funds from which this work was possible. The authors also appreciated the Brazilian Navy Hydrographic Center, and the Brazilian Digital Library for providing the old nautical charts. The authors are also grateful to Brazilian Oceanographic Database (BNDO) for that made the 20th century board sheets available, and the Acquadinâmica for sharing the updated dataset.

3 DISCUSSÃO GERAL

Os resultados fornecem evidências da influência da configuração do canal no delta de maré vazante, forma em planta do canal e assimetria dos lóbulos do delta de maré vazante no processo de transposição do promontório-desembocadura. À medida que o sedimento é redirecionado por meio de processos de onda próximos ao promontório, o transporte em suspensão por ondas é favorecido pelo fluxo enchente. Essa sinergia incorre na acumulação sedimentar em meio ao canal, variando a largura da secção transversal. Com o desenvolvimento do canal, essa diferença na largura (geometria) aumenta a intensidade da corrente vazante, uma vez que o canal é constrito em determinados pontos.

Devido a posição proximal da "zona de deflecção de fluxo", o sedimento é empurrado principalmente em direção aos flancos do canal no lóbulo norte do delta de maré vazante. Isso acontece uma vez que o sedimento empurrado para o lóbulo sul é novamente redirecionado ao canal devido a deflecção do fluxo vazante e dominância do transporte na direção do canal ao redor do promontório. Esse processo aumenta a demanda sedimentar nas porções costeiras mais distantes da entrada da desembocadura. Primeiro, tendo em vista que cria um gradiente de transporte para sul na porção costeira à jusante da desembocadura; segundo uma vez que impede que processos de onda na plataforma do lóbulo sul devolva o sedimento à praia. O mecanismo associado a transposição do promontório-desembocadura, portanto, induz uma reversão do transporte longitudinal ao longo da costa a jusante da desembocadura e inaugura um estágio de armadilhamento de sedimentos no delta de maré vazante.

No cenário de dominância do mecanismo de transposição do promontório-desembocadura através da plataforma de vazante e ao longo do lobo terminal do delta ocorre a expansão de regiões mais afastadas da entrada da enseada ao longo da costa a jusante. Esta descoberta sugere que uma configuração específica de canal, provavelmente devido a formação de um braço sul do canal vazante, e o consequente afastamento em direção ao mar da "zona de deflecção de fluxo", podem ser necessários para que os sedimentos alcancem regiões além da célula de recirculação do delta de maré vazante.

4 CONCLUSÕES GERAIS

O presente trabalho aborda a evolução morfológica da desembocadura da baía da Babitonga através de dados batimétricos extraídos de cartas náuticas antigas, folhas de bordo e levantamento hidrográficos recentes ao longo de 160 anos (1862-1941). Um modelo conceitual de três estágios de evolução morfológica de desembocaduras controladas por promontório é apresentado, considerando a transposição sedimentar do promontório e desembocadura como um processo conjectural único, e considerando mudanças na orientação do fluxo vazante no delta de maré vazante.

A "zona de deflexão de fluxo" é proposta para designar a região onde o fluxo de vazante tende a ser defletido de regiões dominadas pelos processos de refração de onda devido a presença do promontório. A mudança na posição da "zona de deflexão do fluxo", ora mais próximo da costa, ora deslocada em direção ao mar, implica no realinhamento da conexão do fluxo vazante com o delta da maré vazante, afetando o mecanismo dominante de transposição sedimentar.

Trabalhos futuros devem empregar modelagem de longo prazo baseada em processos, abordando a morfodinâmica das desembocaduras controladas por promontórios. Além disso, é crucial considerar a frequência crescente de tempestades e mudanças no clima das ondas em estudos futuros que abordem a evolução das entradas.

5. CONTRIBUIÇÕES CIENTÍFICAS

As principais contribuições científicas proveniente deste trabalho são:

(1) Um modelo conceitual que associa os mecanismos de transposição sedimentar de promontório e desembocadura é apresentado.

(2) Conjuntos de dados batimétricos históricos abrangem um período de 160 anos (1862-1941).

(3) A orientação do fluxo de vazante no delta de maré vazante afeta o mecanismo associado de transposição sedimentar de promontório e desembocadura.

(4) A transposição sedimentar de promontório e desembocadura atraves do transporte para o canal ocorre devido a migração do canal para jusante.

(5) A formação de um braço de vazante orientado na direção do promontório favorece a transposição sedimentar através do lobo terminal do delta de vazante.

REFERÊNCIAS

AB RAZAK, Mohd Shahrizal Bin. **Natural Headland Sand Bypassing**: towards identifying and modelling the mechanisms and processes. Orientador: Dano Roelvink. 2015. 188 f. Tese (Doctoral thesis in Civil Engineering and Geosciences, Hydraulic Engineering) – Gradute Program in Engineering, Technical University of Delft, Delft, 2015. Disponível em: https://repository.tudelft.nl/islandora/object/uuid:4b126111-3f1b-4986-949e-4a174ebf7322?collection=research. Acesso em: 19 nov. 2023.

ALVES, José Henrique Gomes de Mattos. **Refração do espectro de ondas oceânicas em águas rasas**: aplicações para a região costeira de São Francisco do Sul, SC. Orientador: Eloi Melo Filho. 1996. 89 f. Dissertação (Mestrado em Engenharia Ambiental) – Programa de Pós Graduação em Engenharia Ambiental, Centro Tecnológico, Universidade Federal de Santa Catarina, Florianópolis, 1996. Disponível em: https://repositorio.ufsc.br/xmlui/handle/123456789/76959. Acesso em: 19 Nov. 2023.

AMANTE, Christopher J.; EAKINS, Barry W. Accuracy of interpolated bathymetry in digital elevation models. **J. Coast. Res.**, Charlotte, v. 76, n. 1, p. 123-33, dez. 2016. Disponível em: http://dx.doi.org/10.2112/si76-011.

ANGULO, Rodolfo J.; SOUZA, Maria C.; LAMOUR, Marcelo R.. Coastal erosion problems induced by dredging activities in the navigation channel of Paranaguá and São Francisco do Sul Harbor, Southern Brazil. **J. Coast.Res.**, Charlotte, v. 39, n. 1, p. 1801-3, jan. 2006.

ARCMAP. **Slope**. 2021. Disponível em: https://desktop.arcgis.com/en/arcmap/latest/tools/spatial-analyst-toolbox/slope.htm. Acesso em: 19 nov. 2023.

AUBREY, David. G.; SPEER, Paul. E. Updrift migration of tidal inlets. **J. Geol.**, Chicago, v. 92, n. 5, p. 531-45, set. 1984.Disponível em: http://dx.doi.org/10.1086/628890.

BERNSTEIN, David J.; FREEMAN, Christopher W.; SUMNERS, Benjamin W.; MITASOVA, Helena. Modern techniques for improved topo/bathy elevation modeling of tidal inlets. *In*: U.S. HYDRO 2011, 1., 2011, Tampa, FL. **Conference Paper.** Tampa, FL: US HIDRO, 2011. Disponível em: https://www.researchgate.net/profile/Christopher-Freeman-8/publication/320908193_MODERN_TECHNIQUES_FOR_IMPROVED_TOPOBATHY_ELEVATION_MODELING_OF_TIDAL_INLETS/links/5a01cd9da6fdcc232e30aaac/MODERN-TECHNIQUES-FOR-IMPROVED-TOPO-BATHY-ELEVATION-MODELING-OF-TIDAL-INLETS.pdf. Acesso em: 19 nov. 2023.

BRASIL. **Projeto de revitalização e reestruturação das praias do Município de Itapoá – SC através de um sistema de proteção costeira.** Rio de Janeiro, 2019. Disponível em: https://www.gov.br/dnit/pt-br/assuntos/planejamento-e-pesquisa/instituto-nacional-de-pesquisas-hidroviarias. Acesso em 20 ago. 2022.

BRASIL. Biblioteca Nacional Digital. **Brasília**. 2023. Disponível em: https://bndigital.bn.gov.br/. Acesso em: 19 nov. 2023.

BYRNES, Mark R.; BERLINGHOFF, Jennifer L.; GRIFFEE, Sarah F. **Sediment Dynamics in Mobile Bay, Alabama:** Development of an Operational Sediment Budget. Alabama, 2013. Disponível em: https://www.mobilebaynep.com/images/uploads/library/mobile_bay_sediment_budget_final_report_plus_appendices_032013.pdf. Acesso em: 19 nov. 2023.

CALLIARI, Lauro J.; WINTERWERP, Johan C., FERNANDES, Elisa H.L, CUCHIARA, C. Debora; VINZON, B. Susana; SPERLE, Marcelo; HOLLAND, Todd. Fine grain sediment transport and deposition in the Patos Lagoon–Cassino beach sedimentary system. **Cont. Shelf Res.**, Amsterdam, v. 29, n. 3, p. 515-29, mar. 2009. Disponível em: http://dx.doi.org/10.1016/j.csr.2008.09.019.

CAMARGO, José Maurício. **Litoral do estado de Santa Catarina, Brasil:** Promontórios rochosos, comportamento da linha de costa e processo de transposição sedimentar. Orientador: Antonio Henrique da Fontoura Klein. 2020. 112 f. Tese (Doutorado em Geografia) – Programa de Doutorado em Geografia, Centro de Filosofia e Ciências Humanas, Universidade Federal de Santa Catarina, Florianópolis, 2020. Disponível em: https://repositorio.ufsc.br/handle/123456789/219537. Acesso em: 19 nov. 2023.

CREMER, Marta. J. O estuário da Baía da Babitonga. *In*: CREMER, Marta. J; MORALES, Paulo. R.D.; OLIVEIRA, Therezinha. M. N. (orgs.). **Diagnóstico ambiental da Baía da Babitonga**. Joinville: Editora Univille, 2006. p. 15-19.

DAVIS, Richard A.; HAYES, Miles O. What is a wave-dominated coast? **Mar. Geol.** Amsterdam., v. 60, n. 1-4, p. 313-29, ago. 1984. Disponível em: http://dx.doi.org/10.1016/0025-3227(84)90155-5.

DRONKERS, J. Tidal asymmetry and estuarine morphology. **Nethe. J. Sea Res.**, Amsterdam, v. 20, n. 2-3, p. 117-31, ago. 1986. Disponível em: http://dx.doi.org/10.1016/0077-7579(86)90036-0.

ELIAS, Edwin P.L.; PEARSON, Stuart G.; VAN DER SPEK, Ad J. F.; PLUIS, Stefan. Understanding meso-scale processes at a mixed-energy tidal inlet: ameland inlet, the netherlands: implications for coastal maintenance. **Ocean Coast. Manag.**, Amsterdam, v. 222, n. 2-5, p. 1-16, maio 2022. Disponível em: http://dx.doi.org/10.1016/j.ocecoaman.2022.106125.

ELIAS, Edwin P.L.; SPEK, Ad J.F. van Der. Long-term morphodynamic evolution of Texel Inlet and its ebb-tidal delta (The Netherlands). **Mar. Geol.** Amsterdam, v. 225, n. 1-4, p. 5-21, jan. 2006. Disponível em: http://dx.doi.org/10.1016/j.margeo.2005.09.008.

ELSTON, Susan Anne. **Secondary circulation in a sinuous coastal plain estuary**. Orientador: Jackson Blanton. 2005. 294 f. Dissertação (Master in Philosophy In Earth And Atmospheric Sciences) - School of Earth and Atmospheric Sciences, Georgia Institute of Technology, Atlanta, 2005. Disponível em: https://www.proquest.com/docview/304998687?pq-origsite=gscholar&fromopenview=true. Acesso em: 19 nov. 2023.

FAMILKHALILI, Ramin.; TALKE, Stefan. A. The effect of channel deepening on tides and storm surge: a case study of Wilmington, NC. **Geophys. Res. Lett.** Hoboken.**,** v. 43, n. 17, p. 9138-47, set. 2016. Disponível em: http://dx.doi.org/10.1002/2016gl069494.

FITZGERALD, Duncan M. Interactions between the Ebb-Tidal Delta and Landward Shoreline: price inlet, South Carolina. **J. Sediment. Res.** Mc Lean, v. 54, n. 4, p. 1303-18, jan. 1984. Disponível em: http://dx.doi.org/10.1306/212f85c6-2b24-11d78648000102c1865d.

FITZGERALD, Duncan M. Shoreline erosional-depositional processes associated with tidal inlets. BOWMAN, Malcolm J. (org). **Hydrodynamics and sediment dynamics of tidal inlets**: lecture notes on coastal and estuarine studies. New York: Springer, 1988. p. 186-225.

FITZGERALD, Duncan M.; KRAUS, Nicholas C.; HANDS, Edward B. **Natural mechanisms of sediment bypassing at tidal inlets**. 1.ed. Vicksburg: U.S. Army Corps of Engineers, 2000.

FITZGERALD, Duncan. M. Sediment bypassing at mixed energy tidal inlets. *In:* COSTAL ENGINEERING CONFERENCE, 18., 1982. **Proceedings of the Eighteenth Coastal Engineering Conference.** [*S.l.*]., 1982.

FITZGERALD, Duncan. M; ILYA, Buynevich V.; FENSTER, Michael S.; MCKINLAY Paul A. Sand dynamics at the mouth of a rock-bound, tide-dominated estuary. **Sediment. Geol.**, Amsterdam, v. 131, n. 1-2, p. 25-49, mar. 2000. Disponível em: http://dx.doi.org/10.1016/s0037-0738(99)00124-4.

FRIEDRICHS, Carl T.; AUBREY, David G.. Tidal propagation in strongly convergent channels. **J. Geophys. Res.** Flórida, v. 99, n. 2, p. 3321-36, fev. 1994. Disponível em :http://dx.doi.org/10.1029/93jc03219.

HAYES, Miles O. Barrier Island morphology as a function of tidal and wave regime. *In*: LEATHERMAN, Stephen P. (org.). **Barrier Islands**. New York: Academic Press, 1979. p. 1-27.

HEIN, Christopher J.; SHAWLER, Justin; CAMARGO, José Maurício; KLEIN, Antonio H.D.F.; TENEBRUSO, Christopher; FENSTER, Michael S. The role of coastal sediment sinks in modifying longshore sand fluxes: Examples from the coasts of southern Brazil and the Mid-Atlantic USA. *In:* COASTAL SEDIMENTS, 9., 2019, Tampa/St. Pete, Florida. **Proceedings of the Nineth International Conference**. Hackensack, NJ: WORLD SCIENTIFIC, 2019.

HENRICO, Ivan. Optimal interpolation method to predict the bathymetry of Saldanha Bay. **Transactions In Gis.,** Stellenbosch, v. 25, n. 4, p. 1991-2009, ago. 2021.
HICKS, D. Murray; HUME, Terry M. Morphology and size of ebb tidal deltas at natural inlets on open-sea and pocket-bay coasts, North Island, New Zealand. **J. Coast. Res.** Charlotte, [S.L.] p. 47-63. jan. 1996.

JACKSON, Chester W. **Analyzing moving boundaries using R**. Disponível em: https://ambur.r-forge.r-project.org/. Acesso em: 19 nov. 2023.

JACKSON, Chester W.; ALEXANDER, Clark R.; BUSH, David M. Application of the AMBUR R package for spatio-temporal analysis of shoreline change: Jekyll Island, Georgia, USA. **Computers Geosciences.**, Amsterdam, v.41, n.4, p. 199-207, abr. 2012. Disponível em: http://dx.doi.org/10.1016/j.cageo.2011.08.009.

JAY, David A.; LEFFLER, Keith; DEGENS, Sebastian. Long-Term Evolution of Columbia River Tides. **J. Waterw. Port. Coast. Ocean Eng.**, Illinois, v. 137, n. 4, p. 161-211, jul. 2011.

JOHNSTON, Kevin; HOEF, Jay M. Ver; KRIVORUCHKO, Konstantin; LUCAS, Neil. **Using ArcGIS™ Geostatistical Analyst**. Redlands: Esri, 2001. Disponível em: https://downloads2.esri.com/support/documentation/ao_/Using_ArcGIS_Geostatistical_Analyst.pdf.Acesso em: 19 nov. 2023.

KLEIN, Antonio H.D.F.; VIEIRA DA SILVA, Guilherme; TABORDA, Rui; SILVA, Ana P.; SHORT, Andrew D. Headland bypassing and overpassing: form, processes and applications. *In*: JACKSON, Derek W.T.; SHORT, Andrew (org.). **Sandy Beach Morphodynamics**. Amsterdam: Elsevier, 2020. p. 557-91.

KLEIN, H.D.F; MENEZES, Joao Thadeu. Beach Morphodynamics and Profile Sequence for a Headland Bay Coast. **J. Coast. Res.**, West Palm Beach, v. 17, n. 4, p. 812-835, nov. 2001.

KRIVORUCHKO, Konstantin. Empirical Bayesian Kriging: implemented in arcGIS geostatistical analyst. **Arc. User Fall,** Redlands, v. 15, n. 4, p. 6-10, set. 2012. Disponível em: https://www.esri.com/news/arcuser/1012/files/arcuser59/arcuser59.pdf. Acesso em: 19 nov. 2023.

LENSTRA, Klaas J. H.; PLUIS, Stefan; RIDDERINKHOF, Wim; RUESSINK, Gerben; VAN DER VEGT, Maarten. Cyclic channel-shoal dynamics at the Ameland inlet: the impact on waves, tides, and sediment transport. **Ocean Dynamics**, Berlin, v. 69, n. 4, p. 409-25, fev. 2019. Disponível em: http://dx.doi.org/10.1007/s10236-019-01249-3.

LEUVEN, Jasper Robrecht Frans Willem. **Bar and channel patterns in estuaries**. Orientador: Maarten Kleinhans. 2019. 264 f. Thesis (Doctoral Thesis in Geosciences) – Graduate Program of the Faculty of Geosciences, University of Utrecht, Utrecht, 2019. Disponível em: https://dspace.library.uu.nl/handle/1874/379901. Acesso em: 19 nov. 2023.

LI, Jin; HEAP, Andrew D. A review of comparative studies of spatial interpolation methods in environmental sciences: performance and impact factors. **Ecol. Inform.**, Paris., v. 6, n. 3-4, p. 228-41, jul. 2011. Disponível em: http://dx.doi.org/10.1016/j.ecoinf.2010.12.003.

MARINHA DO BRASIL. **Banco Nacional de Dados Oceanográficos**. Brasília, 2023. Disponível em: https://www.marinha.mil.br/chm/bndo. Acesso em: 19 nov. 2023.

NOERNBERG, Mauricio A.; RODRIGO, Pedro A.; LUERSEN, David M. Seasonal and fortnightly variability of the hydrodynamic regime at Babitonga Bay, Southern of Brazil. **Reg. Stud. Mar. Sci.**, Amsterdam, v. 40, n. 18, p. 1-15, nov. 2020. Disponível em: http://dx.doi.org/10.1016/j.rsma.2020.101518.

O'Brien, Morrough. P., Estuary tidal prisms related to entrance area . Civil Eng., [*S.l.*], v. 1, n. 8, p. 738-9, Jan. 1931.

OERTEL, George F. Ebb-tidal deltas of Georgia Estuaries. *In*: OERTEL, George F.(org.) **Estuarine Research**. South Carolina: Academic Press, 1975. p. 267-76.

PHILIP, George M.; WATSON, David. F. A precise method for determining contoured surfaces. **Aust. Pet. Explor. Associ. J.,** Amsterdam, v. 22, n. 1, p. 205-212, jan. 1982. Disponível em: http://dx.doi.org/10.1071/aj81016.

PIANCA, Cassia; HOLMAN, Rob; SIEGLE, Eduardo. Mobility of meso-scale morphology on a microtidal ebb delta measured using remote sensing. **Mar. Geol.**, Amsterdam, v. 357, n. 1, p. 334-43, nov. 2014. Disponível em: http://dx.doi.org/10.1016/j.margeo.2014.09.045.

PULLIG, Mariane C; Klein, Antonio H. D. F.; Pool, Lais S. F.; TOMASI, Marcos F.; MENEZES, João Thadeu; ALVES, Deivid C. L. Babitonga Bay: 80 years of morphological analysis (1940-2021) of the channel and ebb tidal delta. *In*: COASTAL SEDIMENTS, 10., 2023, New Orleans, LA. **Proceedings of the Coastal Sediments 2023**. Hackensack, NJ: WORLD SCIENTIFIC, 2023. p. 1415-1425.

DUARTE, João; TABORDA, Rui; RIBEIRO, Monica., Evidences of headland sediment bypassing at Nazaré Norte Beach, Portugal. *In*: COASTAL SEDIMENTS, 9., 2019, Tampa/St. Pete, Florida. **Proceedings of the Nineth International Conference**. Hackensack, NJ: WORLD SCIENTIFIC, 2019. p. 2709–272.

RALSTON, David K.; TALKE, Stefan; GEYER, Rockwell; AL-ZUBAIDI, Hussein A. M.; SOMMERFIELD, Christopher K. Bigger tides, less flooding: effects of dredging on barotropic dynamics in a highly modified estuary. **J. Geophys. Res.: Oceans,** Hoboken**,** p. 196-211. 2019 Disponível em: https://agupubs.onlinelibrary.wiley.com/doi/epdf/10.1029/2018JC014313. Acesso em: 11 nov. 2023.

RIBEIRO, Mónica Sofia Afonso. **Headland sediment bypassing processes**. Orientadores: Rui Taborda e Aurora Bizarro. 2017. 210 f. Tese (Doutorado em Geologia) – Programa de Pós Graduação em Geologia da Faculdade de Ciências, Universidade de Lisboa, Lisboa, 2017. Disponível em: https://www.proquest.com/docview/2063368055?fromopenview=true&pq-origsite=gscholar&parentSessionId=NwOjGu8E%2FEegXEuuDIXOdMSuj6mpdf%2Fz8ZEqT8hGK2U%3D. Acesso em: 19 nov. 2023.

SHORT, Andrew. D.; MASSELINK, Gerd. Embayed and structurally controlled beaches. *In*: Short, Andrew. D. (org.). **Handbook of beach and shoreface morphodynamics**. New Jersey: John Wiley & Sons, 1999. p. 230-49.

SIEGLE, Eduardo; ASP, Nils E. Wave refraction and longshore transport patterns along the southern Santa Catarina coast. **Braz. J. Oceanogr.** São Paulo, v. 55, n. 2, p. 109-20, jun. 2007. Disponível em: http://dx.doi.org/10.1590/s1679-87592007000200004. Acesso em: 15 jan. 2019.

VIEIRA DA SILVA, Guilherme; TOLDO JR, Elírio E.; Klein, Antonio H. D. F.; SHORT, Andrew D.; WOODROFFE, Colin D. Headland sand bypassing — quantification of net sediment transport in embayed beaches, Santa Catarina Island North Shore, Southern Brazil. **Mar. Geol.**, Amsterdam, v. 379, n. 1, p. 13-27, set. 2016. Disponível em: http://dx.doi.org/10.1016/j.margeo.2016.05.008.

SILVEIRA, Lucas F.; BENEDET, Lindino; SIGNORIN, Morjana; BONANATA, Rafael. Evaluation of the relationships between navigation channel dredging and erosion of adjacent beaches in Southern Brazil. In: INTERNATIONAL CONFERENCE ON COASTAL ENGINEERING, 33, 2012, Santander, SD. **Proceedings of the thirty-third International Conference on Coastal Engineering**. Santander, SD: COASTAL ENGINEERING RESEARCH COUNCIL, 2012.

SOUZA, Maria C.; ANGULO, Rodolfo J.; PASSENDA, Luiz C. R. Evolução paleogeográfica da planície costeira de Itapoá, litoral norte de Santa Catarina. **Rev. Bras. Geo.,** Curitiba , v. 31, n. 2, p. 223-30, jun. 2001.Disponível em:. http://dx.doi.org/10.25249/0375-7536.2001312223230.

SPEER, Paul E.; AUBREY, David G. A study of non-linear tidal propagation in shallow inlet/estuarine systems Part II: theory. **Estuar. Coast. and Shelf Sci.**, Amsterdam, v. 21, n. 2, p. 207-24, ago. 1985. Disponível em http://dx.doi.org/10.1016/0272-7714(85)90097-6.

TROMBETTA, Thaísa. B.; MARQUES, Wiliam C.; GUIMARÃES, Ricardo C.; COSTI, Juliana. An overview of longshore sediment transport on the Brazilian coast. **Reg. Stud. Mar. Sci.**, Amsterdam, v. 35, n. 1, p. 101099, mar. 2020. Disponível em: http://dx.doi.org/10.1016/j.rsma.2020.101099.

TRUCCOLO, Eliane. C.; SCHETTINI, Carlos. A. Marés astronômicas na baía da Babitonga, SC. **Braz. J. Aquat. Sci. Technol.**, Itajaí, v. 3, n. 1, p. 57-66, out. 2010. Disponível em: http://dx.doi.org/10.14210/bjast.v3n1.p57-66.

VELASQUEZ-MONTOYA, Liliana; OVERTON, Margery F.; SCIAUDONE, Elizabeth J. Natural and anthropogenic-induced changes in a tidal inlet: morphological evolution of oregon inlet. **Geomorphol.**, Amsterdam, v. 350, n. 10, p. 68-71, fev. 2020. Disponível em: http://dx.doi.org/10.1016/j.geomorph.2019.106871.

VIEIRA, Celso V.; HORN FILHO, Norberto O.; BONETTI, Carla V.D.H.C.; BONETTI, Jarbas. Caracterização morfosedimentar e setorização do complex estuarino da Baía de Babitonga/ SC. **Bol. Parana. Geociências**, Curitiba, v. 62, n. 1, p. 85-105, dez. 2008. Disponível em: http://dx.doi.org/10.5380/geo.v62i0.12783.

WALTON, Todd. L..; ADAMS, William. D. Capacity of inlet outer bars to store sand. *In*: INTERNATIONAL CONFERENCE ON COASTAL ENGINEERING, 15., 1976, Honolulu, HL. **Proceedings of the Fifteenth International Conference on Coastal Engineering**. New York, NY: AMERICAN SOCIETY OF CIVIL ENGINEERS, 1976.

ZWAMBORN, J.A.; GRIEVE, G. Wave attenuation and concentration associated with harbour approach channels. *In*: COASTAL ENGINEERING**,** [*S.l.*]., 1974, Copenhagen, DE.

Coastal Engineering Proceedings, Reston, USA: COASTAL ENGINEERING RESEARCH COUNCIL, 1974.

APÊNDICE A – INTERPOLATION SETTING

The autocorrelation parameters in EBK method were automatically calculated using measured and simulated data, including the radius of searching (Krivoruchko, 2012). The number of semivariograms simulated for each subset, and the number of points in each subset were kept at 100. The neighborhood type parameter chosen was the Standard Circular. The remain parameters Overlap factor and Angle were kept in their default value of one and zero. The decision not to impose a specific direction for interpolation when using the EBK method relies on the method's capability to develop a semivariogram for each spatial domain. Hence, it was chosen not to enforce autocorrelation in a particular direction, allowing correlation models (semivariograms) to be generated according to the spatial variations within each subset. Different semivariogram types (Linear, Power, and Thin Plate Spline) were examined, and the one associated with the lowest Root-Mean-Square Error and Root-Mean-Square Standardized Error closest to 1 was selected. The semivariogram type, the number of neighbors, and the sector type applied for each dataset are detailed in Supplementary Table I.

When applying Ordinary Kriging, each dataset was detrended by removing the surface based on the polynomial order resulted from the trend global analysis. The function (Exponential, Gaussian) that minimized the goodness of fit was selected as the kernel to fit the surface. The range of each dataset was used as the major semiaxis of the search ellipse, while the minor axis was adjusted to half the value of the range. The dataset directional trend (in degrees from North) observed in the trend analysis was used to orientate the search ellipse. The remaining input parameters - maximum and minimum neighbors, neighborhood type, sector type, and anisotropy factor - were kept at their default settings. After the trend removal, the residual data was used to perform the interpolation. As the autocorrelation modeling and global trend analysis were most likely unable to represent short-range variations, the results obtained with them were not considered during the residual data interpolation. Instead, an optimization function was chosen to determine the setting parameters. Then, the polynomial trend was reincorporated to calculate the predicted map.

In the context of Inverse Distance Weighting (IDW), the power value parameter was selected using the optimizing function, that identifies the weighting factor that minimizes the mean absolute error (Philip and Watson, 1982; Watson and Philip, 1985). The length and

orientation (in degrees from North) of the search ellipse major semiaxis were filled using the dataset's range and trend angle, respectively. The neighborhood type was selected as standard and the number of neighbors was limited within 10 (min) and 15 (max).

Table 1 – EBK setting parameters

Dataset year	Semivariogram type	Sectors	Minimum neighbors	Maximum neighbors	Radius of search circle
1862	Power	8 sectors	8	8	115
1941	Thin Plate Spline	8 sectors	2	5	75
1972	Thin Plate Spline	4 sectors with 45° offset	8	8	114
1981	Thin Plate Spline	1 sector	64	64	140
1995	Power	8 sectors	8	8	100
2020/2021	Power	4 sectors with 45° offset	2	5	52

APÊNDICE B – METHODS COMPARISON

The performances of Ordinary Kriging, the EBK, and the IDW models are shown in Table 2.

Table 2 – Comparison of EBK , Ordinary Kriging, and IDW performance on representing Babitonga Inlet's terrain

Dataset year	Depth range (m)	Density (samples/km²)	RMSE (m) IDW	RMSE (m) OK	RMSE (m) EBK
1862	(-27.4 - 0)	7	2.66	1.60	1.55
1941	(-30 - 0)	8	2.56	1.47	1.37
1972	(-28 - 0)	5	2.63	1.51	1.54
1981	(-21.2 - 0)	100	0.54	0.49	0.46
1995	(-28.5 - 0)	600	0.64	0.58	0.44
2020	(-29 - 0)	160	0.28	0.35	0.22
2021	(-29 - 0)	2120	0.41	0.11	0.11

All three tested methods presented an increase in RMSE as sample density dataset decreased while the dataset range variation showed no relationship with the performance of any of the methods. This result differs from those reported by Li & Heap (2011) that concluded based on 53 studies that sample density does not significantly impact the performance of Ordinary Kriging and IDW methods. According to these authors, sample density effects are dominated by data variability in method performance. Nevertheless, the results indicating the dominant effect of sample density on methods performance is aligned with those from Henrico (2021), who associated the improvement of Ordinary Kriging and IDW interpolators

performance in representing the bathymetry of Saldanha Bay with increased sample density datasets.

The EBK Method was selected to generate the standardized rasters. While the Ordinary Kriging and the EBK methods showed minor differences in its results regarding the quantitative analysis, it´s possible to verify in Figure 9 the closest representation of the original features depicted in the nautical chart by the EBK method. The EBK method resulted in a more accurate capturing of the dredged channel outline, it´s connection with the main ebb channel, the morphology of the shallow regions, and the presence of a secondary flood channel in front of the headland. The cross-validation method results indicate that the geostatistical models outperformed IDW in predict the Babitonga Inlet bathymetry, despite of the distinct sample densities and data variability in each tested subset. Particularly, the superior performance of the EBK over the Ordinary Kriging and IDW methods in reconstruct Babitonga inlet's features contours can be attributed to the EBK method capability to account for the non-stationary nature of the terrain (Krivoruchko, 2012). In classical Kriging method (Ordinary Kriging), unsampled sites are estimated using a single semivariogram based on the entire sampled area, while assumes that the variable's mean varies according to a single trend. In contrast, the EBK method utilizes the data variation across the terrain to determine spatial domains and specific semivariograms for each spatial domain. These semivariograms capture correlated fluctuations that deviate from the spatial domain long-range spatial trend. As a result, the EBK method implements a non-stationary algorithm (Krivoruchko, 2012).

Figure 10 - Performance of the (a) Classical Kriging; (b) EBK and (c) IDW interpolation methods in comparison to Brazilian's Navy 1981 Nautical Chart morphological features (d).

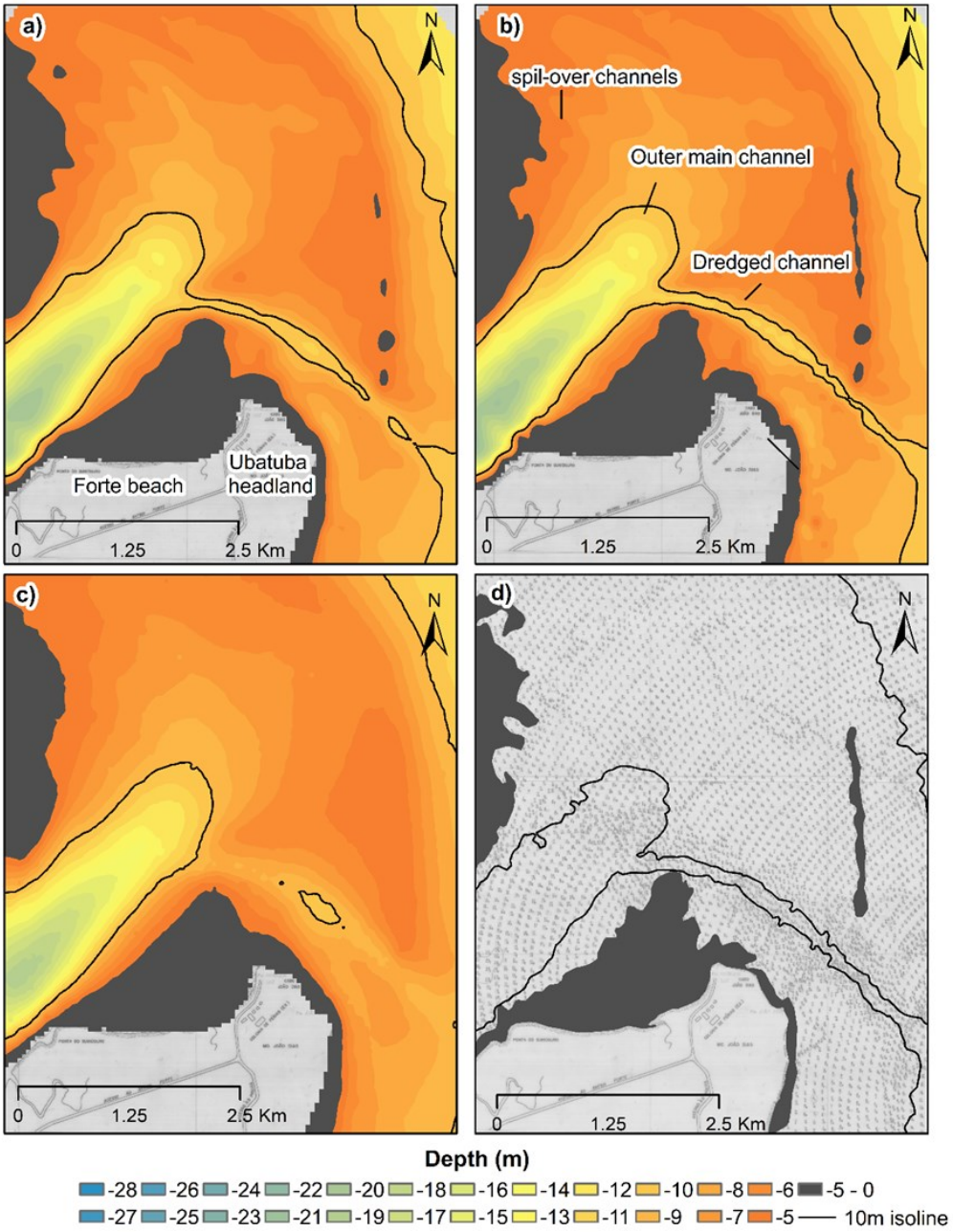

Source: Elaborated by the authors.

The Prediction Standard Error map presented in Figure 10 addresses the variations in the degree of error associated with the EBK Model across the interpolated area. The EBK model outperformed in higher homogeneity data regions, such as the ebb delta platform. However, in areas characterized by higher natural variability, such as the channel, the delta terminal lobe, and the spill-over channels, the method performance declined. The spatial performance of the method was primarily influenced by the natural slopes, that amplified the variation in data,

leading to a reduction in the model's predictive accuracy. Notably, the accuracy of the model decreased in dredged portions and areas adjacent to the boundaries of the Digital Elevation Models, compared to regions with natural slopes. The introduction of abrupt slopes resulting from dredging activities, along with the methodological limitation of data gaps near the coastline, can account for the observed error pattern (see figure 10). Additionally, the IDW method also tends to exhibit less accuracy across high slope areas, as reported by Amante and Eakins (2016). Since the values that should be predicted as local maximum and minimum are leveled closer to the surrounding values, the IDW method has lower skill in interpolating across steeper slopes. Despite that, the study of Henrico (2021) compared Ordinary Kriging and IDW methods and selected the IDW method as the optimal technique for representing the 85 km² terrain of Saldanha Bay. The dataset that showed statistical significantly optimal representation by the IDW method corresponded in density to that of the old nautical charts in this study. Additionally, the data variation in Saldanha Bay (up to 50m) is greater than that found in Babitonga Bay (depth up to 30m). Therefore, the reason for the superiority of the IDW method is not related to higher sample density or lower data variability. In the other hand, Saldanha Bay exhibits a gentler slope in comparison to Babitonga Bay, which could have influenced the performance of the IDW method.

Figure 11 - Spatial variations in EBK model performance for the Brazilian's Navy 1981 Nautical Chart. The contour line was extract from EBK output grid. An 1/3 standard deviation classification was applied to split the groups.

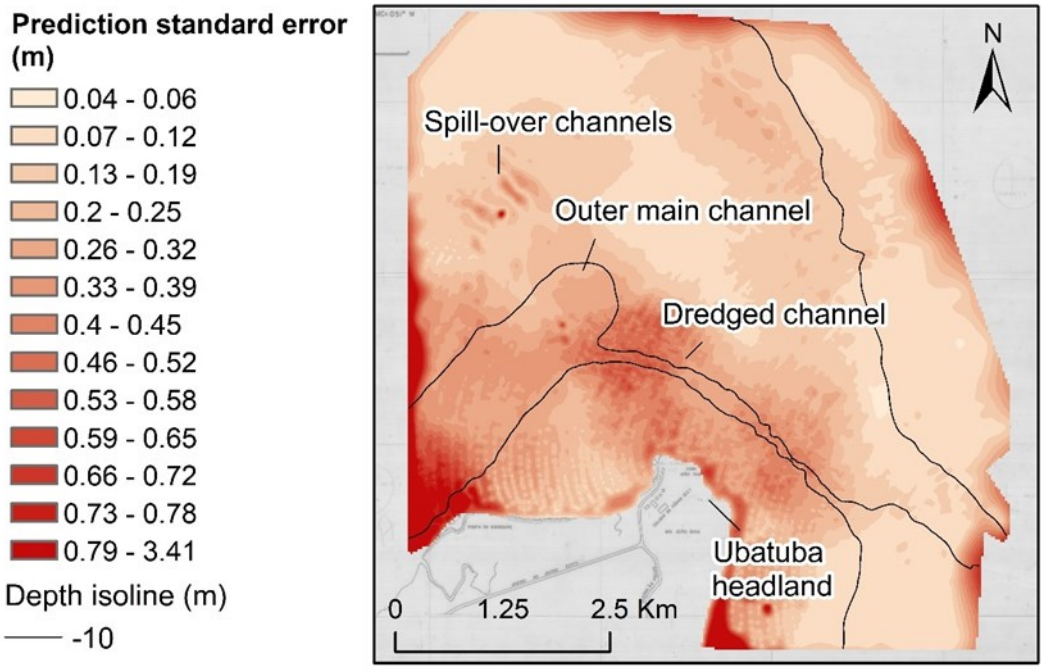

Source: Elaborated by the authors.

APÊNDICE C – DIRECTIONAL TRENDS IN DATA SAMPLING

A hybrid interpolation was employed on the 2021 dataset to minimize the effects of survey lines oversampling and data acquisition in an oblique direction relative to the natural contour of the terrain. The main strategy involved analyzing the directional trend of the isolated feature data and interpolate the feature considering its directional trend. Firstly, the data across the dredged channel was clipped and removed from the original bathymetry and a local trend analysis was performed using solely the data isolated. After, a survey line refinement was employed by creating artificials survey lines through linear interpolation. Subsequently, a regular 50X50m grid was generated by interpolating the along-line data in its main direction using IDW method. Finally, the interpolated data was reincorporated into the clipped inlet bathymetry.

The interpolation artifacts associated with oversampled lines surveyed obliquely to the natural contour direction required the introduction of an anisotropic factor, as anticipated by Bernstein *et al*. (2011), and the employment of a hybrid method. Nevertheless, a few considerations should be addressed regarding the application of the anisotropy factor associated with survey line refinement at inlet environments. Firstly, the refinement using linear interpolation benefited the final raster since it involved a feature modified by human interventions with known maximum depth values. Secondly, interpolating in the direction resulting from the entire dataset trend analysis did not help reduce the surveyed lines-associated artifacts on the predicted map. Since inlets comprise features oriented in several directions due to wind, tides, and wave action, the overall trend analysis was unable to recover the relation between features contour direction and the surveyed lines orientation. Thus, isolating the feature data for anisotropic analysis was crucial to properly detrend the data and reduce the signature of strait survey lines. The interpolation model accuracy is driven by data variation across the surveyed area. In the presence of steeper slope terrain, such as deep channel and tidal flats inlets, this study suggests interpolation should be carried out parallel to the direction presenting lower data variability, i.e., along the natural feature contour, especially in cases where the dataset exhibits a directional trend in data sampling.

APÊNDICE D – RESUMOS DE TRABALHOS APRESENTADOS

Neste tópico são apresentados os resumos aceitos em eventos.

I. IGCP 2023

Babitonga bay 160 years morphological evolution: inlet sedimentary bypassing pathways

Mariane Couceiro Pullig[1], Antonio Henrique da Fontoura Klein[1], Laís Pool da Silva Freitas[2], Marcos Felipe Tomasi[1], João Thadeu de Menezes[3], Deivid Cristian Leal Alves[4]

[1] Federal University of Santa Catarina, University Campus - Trindade, Florianópolis, Santa Catarina, Brazil.
[2]Federal University of Rio Grande do Sul,- Porto Alegre, Rio Grande do Sul, Brazil. -
[3]ACQUADINÂMICA Modelagem e Análise de Risco Ambiental, Balneário Camboriú Santa Catarina, Brazil. -
[4]State University of Mato Grosso do Sul, -Dourados, Mato Grosso do Sul, Brazil. -

Inlets are natural barriers to longshore flux toward downdrift coasts. The way sediment bypasses these inlets can lead to significant morphological changes, ultimately establishing a new morphodynamical equilibrium. Although the mechanisms involved in sediment bypassing at inlets have been described by FitzGerald, Kraus and Hands (2000), the understanding of sediment connectivity and its forcing along large inlet-dominated coasts remains limited. Additionally, the sedimentary process occurring in mesoscale inlet-bay systems is poorly understood due to the need for long-term bathymetric monitoring. In this study, we investigate the formation of bars in the channel and ebb-tidal delta of a mixed energy inlet located in Babitonga bay, southern Brazil. Our primary goal is to identify the secular (1862 – 2021) sedimentary bypassing pathways. We compared the bathymetries from Digital Elevation Models, created through Empirical Bayesian Kriging interpolation method. Hypsometric analysis is also conducted using bathymetric datasets. Historical Bathymetric datasets (compilation years: 1862, 1941, 1972, 1981 and 1995) were obtained from Brazilian Navy's nautical charts while recent datasets (2020 and 2021) were made available through academic cooperation. Our findings indicate that changes in the alignment of the Inlet's throat, as a result

of bar relocation and channel meandering, explain the observed morphological changes in the southern and northern ebb-tidal delta lobes. Those changes also influence the process of bar attaching along the downdrift coast.

Keywords: Meso-scale estuary. Interpolation methods. Ebb tidal delta. Long-term analysis

ANEXO A – HISTORICAL DOCUMENTS COMPRISING THE MORPHOLOGICAL DATABASE OF BABITONGA INLET

Table 3. Title, survey date, authorship, and reference of the historical documents Nautical Charts, Board Sheets, and recent datasets constituting the morphological database utilized in this study.

Title	Bathymetry survey date	Authorship	Reference
South America. East Coast. Coast of Brazil...Entrence of the river São Francisco (do Sul)...1862 [Cartográfico] **Nautical Chart**	1862	United States. Naval Oceanographic Office. Under the custody of Brazilian Library	UNITED STATES. Naval Oceanographic Office. **South America. East Coast. Coast of Brazil...Entrence of the river São Francisco (do Sul)...1862.** Washington [Estados Unidos], 1873. 1 mapa, 62 x 89. Disponível em: http://objdigital.bn.br/objdigital2/acervo_digital/div_cartografia/cart537956/cart537956.jpg. Acesso em: 25 jun. 2021. Disponível em: http://objdigital.bn.br/objdigital2/acervo_digital/div_cartografia/cart537956/cart537956.html. Acesso em: 25 jun. 2021.
Brasil - Costa Sul [Cartográfico] : Porto de São Francisco do Sul 164836 **Nautical Chart**	1941	Brazilian Navy Hydrographic Center. Under the custody of Brazilian Library	BRASIL. Diretoria de Hidrografia e Navegação. **Brasil - Costa Sul:** Porto de São Francisco do Sul. Rio de Janeiro, RJ: Ministério da Marinha, 1941. 1 carta hidrográfica, col, 66 x 95. Disponível em: http://objdigital.bn.br/objdigital2/acervo_digital/div_cartografia/cart164836/cart164pg. Acesso em: 25 jun. 2021.
Brasil - Costa Sul Porto de São Francisco do Sul **Nautical Chart**	1972	Brazilian Navy Hydrographic Center	Digital collection Brazilian Library
1804_02_81 Fundeadouro de São Francisco – Área Bravo **Board Sheet**	1981	Brazilian Navy Hydrographic Center	Brazilian Oceanographic Database

1804_01_81 Barra do Rio São Francisco do Sul **Board Sheet**	1981	Brazilian Navy Hydrographic Center	Brazilian Oceanographic Database
1804_001_95 Canal de acesso ao Porto de São Francisco do Sul **Board Sheet**	1995	Brazilian Navy Hydrographic Center	Brazilian Oceanographic Database
1804_002_95 Canal de acesso ao Porto de São Francisco do Sul **Board Sheet**	1995	Brazilian Navy Hydrographic Center	Brazilian Oceanographic Database
1804_003_95 Canal de acesso ao Porto de São Francisco do Sul **Board Sheet**	1995	Brazilian Navy Hydrographic Center	Brazilian Oceanographic Database
1804_004_95 Bacia de evolução do Porto de São Francisco do Sul **Board Sheet**	1995	Brazilian Navy Hydrographic Center	Brazilian Oceanographic Database
1804_005_95 Porto de São Francisco do Sul Prox. Ilha da Paz **Board Sheet**	1995	Brazilian Navy Hydrographic Center	Brazilian Oceanographic Database
1804_006_95 Porto de São Francisco do Sul Prox. Ilha da Paz **Board Sheet**	1995	Brazilian Navy Hydrographic Center	Brazilian Oceanographic Database

1804_007_95 Prox. do Porto de São Francisco do Sul **Board Sheet**	1995	Brazilian Navy Hydrographic Center	Brazilian Oceanographic Database
CbatimetriaScpar	2020	SCPAR	SCPAR - Santa Catarina Parcerias Porto de São Francisco do Sul (SFS Harbor). Provided by Acquadinâmica Ltd.
BELOV2021	2021	Belov Engenharia Ltd.	SCPAR - Santa Catarina Parcerias Porto de São Francisco do Sul (SFS Harbor). Provided by Acquadinâmica Ltd.